Universidade de Aveiro Departamento de Biologia
2011

CARINA TERESA DOS SANTOS RODRIGUES

LOCAL TRANSLATION OF CANDIDATE mRNAs FOR DOWN'S SYNDROME

TRANSLAÇÃO LOCAL DE mRNAs EM SINDROME DE DOWN

Universidade de Aveiro Departamento de Biologia
2011

CARINA TERESA DOS SANTOS RODRIGUES

LOCAL TRANSLATION OF CANDIDATE mRNAs FOR DOWN'S SYNDROME

TRANSLAÇÃO LOCAL DE mRNAs EM SINDROME DE DOWN

Dissertação apresentada à Universidade de Aveiro para cumprimento dos requisitos necessários à obtenção do grau de Mestre em Biologia Aplicada, realizada sob a orientação científica da Professora Doutora María Luz Montesinos, Professora Titular do Departamento de Fisiologia Médica y Biofisica da Universidade de Sevilha e co-orientação da Professora Doutora Margarida Sâncio da Cruz Fardilha, Professora Auxiliar Convidada da Secção Autónoma de Ciências da Saúde da Universidade de Aveiro.

o júri

Presidente	Professor Doutor António José Arsénia Nogueira Prof. Associado c/ agregação, Departamento de Biologia, Universidade de Aveiro
Orientadora	Professora Doutora Maria Luz Montesinos Prof. Titular, Departamento de Fisiologia Médica y Biofisica, Faculdad de Medicina, Universidad de Sevilla
Co-Orientadora	Professora Doutora Margarida Sâncio da Cruz Fardilha Prof. Auxiliar, Secção Autónoma de Ciências da Saúde, Universidade de Aveiro
Arguente principal	Professora Doutora Rita Maria Pinho Ferreira Prof. Auxiliar Convidado, Departamento de Química, Universidade de Aveiro

Agradecimentos

À María Luz Montesinos pela atenção e amabilidade com que me recebeu no Synaptic Local Translation Lab através do programa Leonardo da Vinci. Todo o conhecimento, incentivo e motivação diária que me transmitiu, fizeram deste trabalho uma experiência extremamente gratificante tanto a nível pessoal como profissional. Muchas Gracias!!

A todos os colegas do Departamento de Fisiología Médica y Biofísica da Universidad de Sevilla, em particular à Alexandra, José, Juanjo, José António María Angeles e Imane.

À Professora Margarida Fardilha, pela disponibilidade, motivação e apoio oferecido durante a redacção desta dissertação.

À minha família, em especial aos meus pais e irmão por todo o amor e apoio incondicional oferecido ao longo de todas as etapas da minha vida.

Ao Célio por todo o amor que me completa e dá força para ultrapassar todas as barreiras.

À Catarina pela amizade e por todos os momentos únicos partilhados ao longo destes anos, dentro e fora do departamento de Biologia.

A todos os meus amigos que sabem que estão e estarão sempre presentes, apesar das minhas ausências.

Palavras-chave Neurónios de hipocampo, translação local, *DSCAM*, pKaede

Resumo

O Síndrome de Down (DS) é a causa genética mais frequente de atraso mental. À semelhança de outros síndromes em que ocorrem deficiências em termos de memória e aprendizagem, as anomalias em especial ao nível das espinhas dendríticas estão também presentes. As espinhas dendríticas exibem rápidas mudanças em número, tamanho, forma e motilidade. Estas mudanças estão associadas à plasticidade sináptica e requerem a síntese de proteínas *in situ*, ou seja, translação local dendrítica. *Down Syndrome Cell Adhesion Molecule* (*DSCAM*) é um dos genes importantes nesta patologia neuronal (DS). Neste trabalho foram analisadas isoformas de *DSCAM* (isoformas 1, 3, 4 e 5) originadas por poliadenilação alternativa e que contem motivos de regulação denominados Cytoplasmic Polyadenylation Element (CPE). Assim, a translação local dendrítica de algumas destas isoformas é regulada pela proteína CPEB. Para visualizar a expressão destas isoformas foram efectuadas construções com a proteína Kaede. Inicialmente esta proteína produz fluorescência em verde e após fotoconversão em vermelho e estimulação sináptica, a nova proteína sintetizada é observada novamente em verde. Neste trabalho foram utilizadas culturas de neurónios de hipocampo, transfectadas com as construções efectuadas com Kaede-*DSCAM*-isoforms e analisadas através de microscopia confocal. Aparentemente, as quatro isoformas de *DSCAM* tem distintos locais de expressão em neurónios. Kaede-*DSCAM*-Isoform 1 é expressa em dendrites e axónios mas não no corpo celular neuronal, enquanto que Kaede-*DSCAM*-Isoform 3 parece ser expressa em todos os compartimentos neuronais. A expressão de Kaede-*DSCAM*-Isoform 4 confere uma morfologia aberrante ao corpo celular neuronal no qual se expressa de forma intensa. Finalmente, a expressão de Kaede-*DSCAM*-Isoform 5 é visualizada na forma de grânulos, em neurites semelhantes a axónios. Apesar da estimulação sináptica não ter sido executada neste trabalho, a utilização de *DSCAM* Kaede-reporters representa uma ferramenta valiosa para a visualização da translação local em culturas neuronais de hipocampo. A aplicação desta metodologia em neurónios de hipocampo de ratos trissomicos Ts1Cje, pode também levar à obtenção de conclusões de extrema importância no que diz respeito ao papel de *DSCAM* em DS.

keywords Hippocampal neurons, local translation, *DSCAM*, pKaede,

Abstract

Down's syndrome (DS) is the most frequent genetic cause of mental retardation. Like in other syndromes involving memory and learning impairment, synaptic structural abnormalities are present, especially at the level of dendritic spines. Dendritic spines undergo rapid changes in number, size, shape and motility. These changes are linked to synaptic plasticity and require in situ protein synthesis, that is, dendritic local translation. *Down Syndrome Cell Adhesion Molecule* (*DSCAM*) is an important gene for DS neuronal pathology. *DSCAM* isoforms analysed in this work (isoforms 1, 3, 4 and 5) are originated by alternative polyadenylation and bear different combinations of regulatory Cytoplasmic Polyadenylation Element (CPE) motifs. Thus, dendritic local translation of some of these isoforms is regulated by CPEB protein. To visualize the local expression of these isoforms, constructions with Kaede protein were made. Kaede protein initially produces green fluorescence, and after irreversible green to red photoconversion and synaptic stimulation, newly synthetized proteins can be observed in green. In this work, hippocampal neuronal cultures were transfected with *DSCAM* Kaede-based reporters and analysed by confocal microscopy. We have found that apparently, the four *DSCAM* isoforms have distinct expression locations in neurons. Kaede-*DSCAM*-isoform 1 is expressed in dendrites and axons but not in cell body whereas Kaede-*DSCAM*-isoform 3 appears to be expressed in all neuronal compartments. Kaede-*DSCAM*-isoform 4 expression seems to confer an aberrant morphological appearance to the neuronal cell body, where it is highly expressed. Finally, expression of Kaede-*DSCAM*-isoform 5 is visualized in form of granules that delineate axon-like neurites. Despite synaptic stimulation of neurons was not performed in this work, *DSCAM* Kaede-based reporters represent a valuable tool for visualizing *DSCAM* local translation in hippocampal neuron cultures. The application of this methodology to trisomic Ts1Cje mouse hippocampal neurons can also lead in the near future to valuable conclusions in what concerns the role of DSCAM in DS.

Contents

List of figures

List of tables

List of abbreviations

AD	Alzheimer's disease
Akt	Non-specific serine/threonine-protein kinase family
APP	Amyloid beta (A4) precursor protein
Arc	Activity-regulated cytoskeleton-associated protein
AS	Alternative splicing
BC1	Brain cytoplasmic 1
BDNF	Brain-derived neurotrophic factor
CAM	Cell adhesion molecule
cCPE	consensus cytoplasmic polyadenylation element
CNS	Central nervous system
CPE	Cytoplasmic-polyadenylation element
CPEB1	Cytoplasmic-polyadenylation element binding protein 1
CPSF	Cleavage and polyadenylation specificity factor
CYFIP1	Cytoplasmic FMR1-interacting protein 1
DIV7	Day 7 in vitro
DS	Down's Syndrome
DSCAM	Down syndrome cell adhesion molecule
DSCR	Down syndrome critical region
DSCR	Down's syndrome critical region
DTE	Dendritic targeting element
eEF2	Eucaryotic translation elongation factor 2
eIF4E	Eukaryotic translation initiation factor
eIF4E-BP	eIF4E-binding protein
ERK	Extracelular signal-regulated kinase
FMR1	Fragile X mental retardation 1
FMRP	Fragile X mental retardation protein
FXS	Fragile X Syndrome
GFP	Green fluorescent protein
Glu	Glutamate
GluR1	Glutamate receptor 1, AMPA receptor sunbunit
GluR2	Glutamate receptor 2, AMPA receptor sunbunit
GluR5	Glutamate receptor 5, AMPA receptor sunbunit
HSA21	Human chromosome 21

Ig	Immunoglobulin
IgSF	Immunoglobulin superfamily
IRS	Internal ribosomal entry sites
IRSp53	Insulin receptor substrate p53
LIMKI	Lim domain kinase 1
LTD	Long-term depression
LTM	Long-term memory
LTP	Long-term potentiation
MAP2	Microtubule-associated protein 2
miRNA	microRNA
MR	Mental Retardation
mRNA	Messenger RNA
MT	Microtubule
mTOR	Mammalian target of rapamycin
ncCPE	nonconsensus cytoplasmic polyadenylation element
NMDA	N-Methyl-D-aspartic acid
NMDAR1	NMDA receptor 1
NT	Neurotrofic
ORF	Open readin frame
PAP	Poly (A) polymerase
PB	Processing body
PBE	Pumilio-binding element
P-bodies	Processing bodies
PDK1/2	Extracellular signal-related kinase 1/2
PI3K	Phosphoinositide 3-kinase
PIKE	PI 3-Kinase Enhancer
PIP3	Phosphatidylinositol 3,4,5-trisphosphate
PLC	phospholipase C
PP2A	Protein phosphatase 2A
PSD	Postsynaptic density
RBP	RNA-binding protein
RNA	Ribonucleic acid
RNP	Ribonucleoprotein particle
RNP	Ribonucleoprotein particles
S6K1	Ribossomal protein S6 kinase 1

SG	Stress granules
SG	Stress granules
tPA	Tissue plasminogen activator
TrkB	Tyrosine kinase receptor B
UTR	Untranslated region
UV	Ultra violet
VDCC	Voltage-dependent Ca2+ Channels
αCaMKII	Calcium/ calmodulin-dependent protein kinase II (α-subunit)
4E-BP1	eIF4E-binding protein 1
5'TOP	5' terminal oligopyrimidine tract

1. Introduction

1.1 Transport and local translation of dendritic mRNAs

The synthesis of a specific protein or functional cohort of proteins at a specific time and place in the cell is required for many cellular functions (Bramham and Wells, 2007).

Neurons are morphologically complex cells. They show a high degree of structural polarization, represented by dendrites, axons and cell bodies that indeed define functional compartments (Fig. 1). These compartments are able to respond to local signals and regulate different cellular processes (Grafstein and Forman, 1980). Local translation of dendritic mRNAs is an example. A descriptive model of neuron morphology and post-transcriptional regulation is shown in the figure 1.

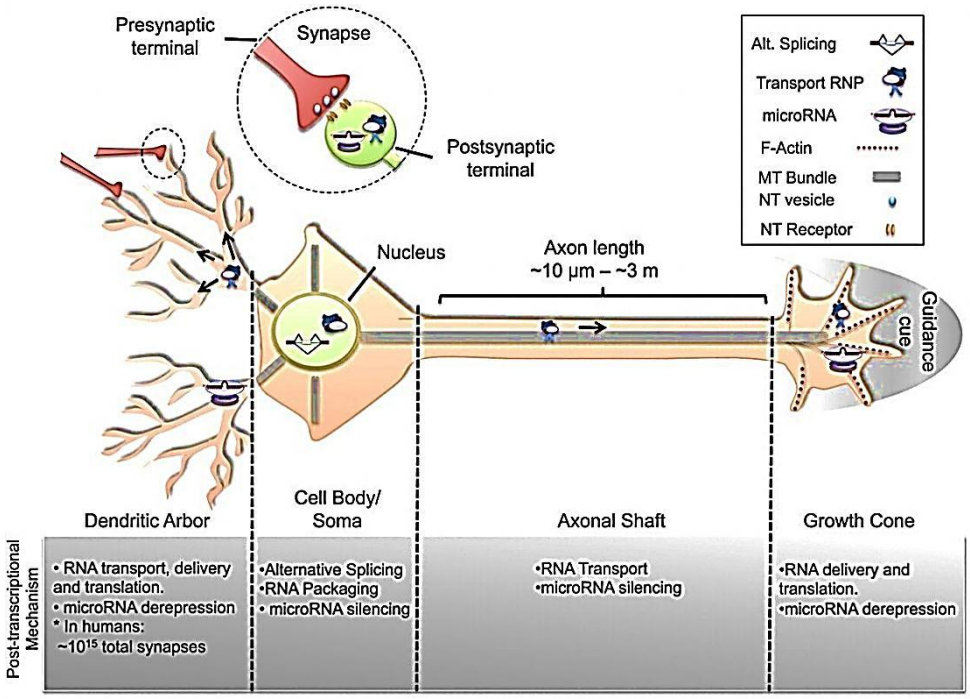

Figure 1: Complexity of neuronal morphology and post-transcriptional regulation.

Typical neuron illustrating four gross neuronal anatomical segments: cell body/soma, axonal shaft, dendritic arbor, and growth cone. Inset shows a synapse, with presynaptic and post-synaptic terminals. The post-transcriptional mechanisms highlighted here are alternative splicing (AS), RNA transport, and miRNA silencing. AS occurs in the nucleus of the cell body, and is important for generating protein isoforms. Following splicing and mRNA maturation, the transcript can be packaged into transport ribonucleoprotein particles (RNPs), repressed by RNA-binding proteins (RBPs) and/or miRNAs, delivered to distal sites of the neuron, and locally translated in response to stimuli. Moreover, miRNAs are involved in finely regulating protein levels throughout the cell (From Van Vactor et al 2010).

In a classical view, mRNA is exported to the cytosol, then it is translated by polyribosomes in the cell body, and the novo proteins are transported to its respective site of action (Van Vactor et al., 2010).

In 1982, Steward and Levy reported for the first time the existence of polyribosome accumulation at the neck of dendritic spines. This observation suggested the possibility that translation occurred not only in the cell body, but also into dendrites (Steward and Levy, 1982).

On the surface of neuronal dendrites there are small protrusions - dendritic spines - where synaptic sites are formed to receive presynaptic signals and transmit mainly excitatory signals (Kirov and Harris, 1999). That mRNA can distribute into both neuronal axons and dendrites is well established. It is also assumed that the synthesis of proteins in the dendrites is regulated by mRNA transport to specific cellular locations (Kim et al., 2005). However, the mechanism by which specific mRNAs are transported is still largely a mystery (Bramham and Wells, 2007, Dictenberg et al., 2008).

From the moment a gene is transcribed, it undergoes a series of post transcriptional regulatory modifications in the nucleus and cytoplasm until its final deployment as a functional protein. Initially, a mRNA is subjected to extensive structural regulation through alternative splicing, which is capable of greatly expanding the protein repertoire by generating, in some cases, thousands of functionally distinct isoforms from a single gene locus. Then, RNA packages into neuronal transport granules as ribonucleoprotein particles (RNPs), stress granules (SGs) and processing bodies (PBs) (Anderson and Kedersha, 2006, Kiebler and Bassell, 2006).

The recognition by RNA-binding proteins and/or microRNAs is capable of restricting protein synthesis to selective locations and under specific input conditions. This ability of the posttranscriptional apparatus to expand the informational content of a cell and control the deployment of proteins in both spatial and temporal dimensions is a feature well adapted for the extreme morphological properties of neural cells (Van Vactor et al., 2010). The figure 2 summarises the main known mechanism responsible for translation control in dendrites.

Regarding the role of local translation, it is now clear that this process is important for dendritogenesis, axonal growth and synaptogenesis during development and for synaptic plasticity in the adulthood.

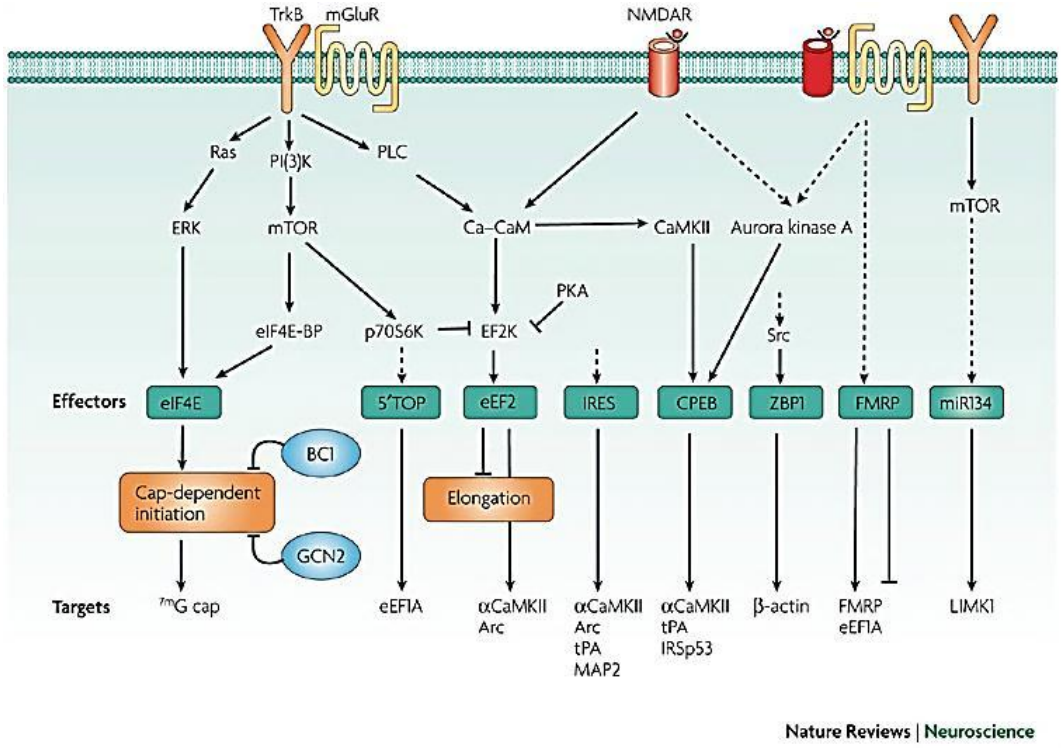

Figure 2: Translation control in dendrites.

The illustration depicts neurotransmitter receptor-coupled pathways that have been implicated in the control of dendritic protein synthesis at excitatory synapses in the mammalian brain (the dotted lines represent unknown signaling pathways) (From Bramham & Wells 2007).

It is widely accepted that most mRNAs are transported into dendrites as part of large RNPs. Although not proven, it is thought that the mRNAs are transported in a translationally dormant state. Therefore, in order for specific mRNAs to be dendritically targeted, they must first be sequestered from the translational machinery in the cytoplasm and organized into RNPs. The sequestration for translation is likely to start in the nucleus, with the binding of proteins that will remain bound to the mRNA on its journey out of the nucleus and into the dendrite (Bramham and Wells, 2007). Phosphorylation of eIF4E is considered the rate-limiting step for the translation of most mRNAs. The phosphorylation of this factor is correlated with enhanced rates of cap-dependent translation, whereas hypophosphorylation is associated with decreased translation (Klann and Dever, 2004, Richter and Sonenberg, 2005). Cap-dependent translation in dendrites is thought to be stimulated by two receptor coupled kinase pathways: extracellular signal-regulated kinase (ERK) signaling, which leads to phosphorylation of eIF4E, and mammalian target of rapamycin (mTOR) signaling, which leads to phosphorylation of eIF4E-binding protein

(eIF4E-BP) and release of eIF4E, which then becomes available for cap binding. Dendritic protein synthesis that affects synaptic plasticity is also controlled at the level of peptide chain elongation. eEF2 is a GTP-binding protein that mediates the translocation of peptidyl-tRNAs from the A-site to the P-site on the ribosome as amino acids are added to the peptide chain. Phosphorylation of eEF2 on Thr56 inhibits eEF2–ribosome binding and arrests elongation (Browne and Proud, 2002, Bramham and Wells, 2007).

In addition to these general mechanisms for controlling local translation rates, there are specific proteins involved in regulating local translation of particular sets of dendritic mRNAs. The most well-known are FMRP and CPEB.

1.1.1 Fragile-X Mental Retardation Protein (FMRP)

FMRP is a selective RNA-binding protein that regulates the local translation of a subset of mRNAs and is likely to be involved in mRNA metabolism in many cell types (Bassell and Warren, 2008). A trinucleotide repeat expansion inactivating the X-linked FMR1 gene, leads to the absence of FMRP, associated with a form of mental retardation called fragile-X syndrome (FXS) (Garber et al., 2006).

In neurons, FMRP is localized to dendrites, and the loss of FMRP results in altered synaptic morphology and plasticity (Bramham and Wells, 2007). The altered synaptic functions are a consequence of excess and dysregulated mRNA translation and loss of protein synthesis-dependent plasticity (Bassell and Warren, 2008).

The regulation of mRNA translation by FMRP is a complicated and poorly defined process (Garber et al., 2006). Even so, and regarding recent reviews that have examined the current understanding of FMRP regulation and function in neurons, two proposed models are shown in the figure 3 and figure 4.

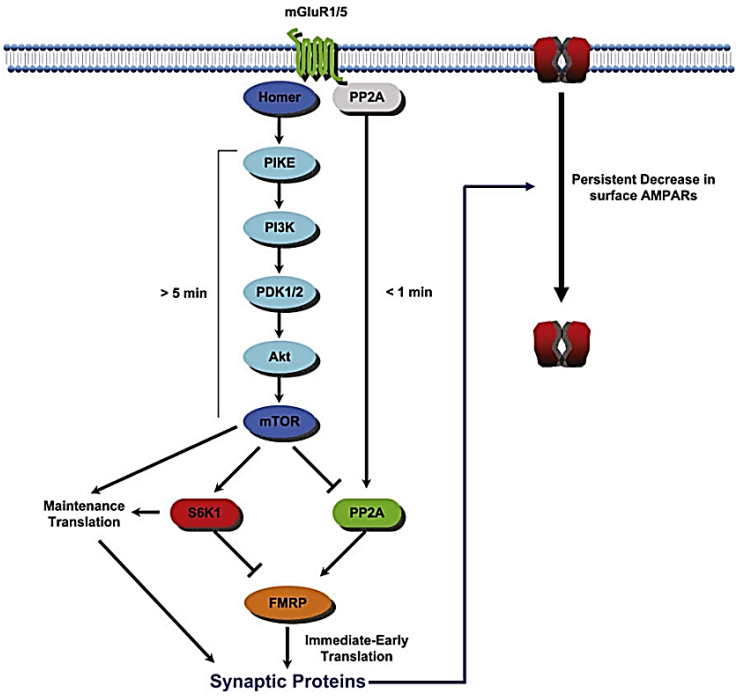

Figure 3: Postsynaptic FMRP Signaling Model.

Following stimulation of Gp1 mGluRs (green), inactive PP2A (gray) is immediately activated (green) and dephosphorylates FMRP (orange), allowing rapid translation of FMRP-associated mRNAs. Within 5 min, mTOR (blue) is activated via a homer cascade, inhibiting PP2A and activating S6K1 (red), leading to FMRP phosphorylation and possible translational inhibition of FMRP target mRNAs. Simultaneously, mTOR activates translation in an FMRP-independent manner, triggering a sustained maintenance of translation. FMRP-dependent and -independent pathways control AMPA receptor internalization and other changes in synaptic function and spine morphology that contribute to synaptic plasticity (From Bassell and Warren, 2008).

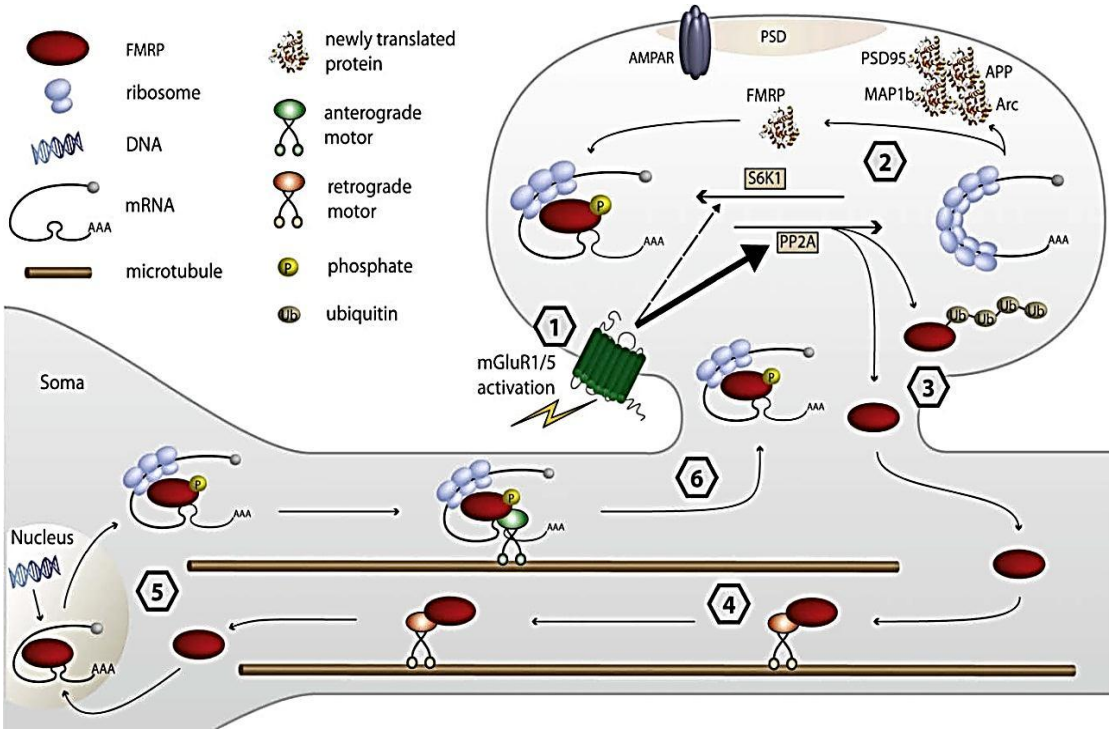

Figure 4: The Stimulated Travels and Function of FMRP throughout the Neuron.

FMRP is in a complex with several translationally arrested mRNAs at the synapse. Following mGluR stimulation, FMRP-target mRNAs are rapidly derepressed, allowing for local translation. A second phase of FMRP-dependent plasticity is shown that involves the subsequent transport of new mRNAs from the cell body into dendrites. The model shown here illustrates translational repression at the level of elongation, as suggested by Ceman et al. (2003). The translational activation and repression of mRNA is regulated by a PP2A/S6K1 signaling module (Narayanan et al., 2007, Narayanan et al., 2008) (see Figure 3). (1) Upon mGluR1/5 activation, PP2A is rapidly activated and dephosphorylates FMRP, thereby allowing for (2) local translation of proteins that affect AMPAR trafficking, i.e., PSD-95, Arc, Map1b, and App (Hou et al., 2006, Westmark and Malter, 2007, Park et al., 2008, Waung et al., 2008). Following mGluR activation, FMRP is rephosphorylated by S6K1 with slower kinetics, leading to translational repression. (3) FMRP can also be ubiquitinated following mGluR stimulation, and its proteosome-dependent degradation is necessary for mGluR-LTD (Hou et al., 2006). The local degradation of FMRP may contribute to local protein synthesis underlying mGluR-LTD. A mechanism of local FMRP degradation may be balanced by its synthesis. FMRP is synthesized in synaptoneurosomes upon mGluR activation (Weiler et al., 1997), which may provide a feedback mechanism to restore translational repression. Upon mGluR stimulation, (4) there may be a retrograde signal that leads to the transport of new FMRP-associated mRNAs from the soma. The active bidirectional transport of FMRP granules in dendrites has recently been described (Dictenberg et al., 2008). This model speculates that FMRP itself may traffic from the synapse to the cell body and/or nucleus, where it may complex with new target mRNAs, and return to the activated synapse. (5) In that FMRP can shuttle into

the nucleus, it will be interesting to assess whether nucleocytoplasmic trafficking is regulated by mGluR signaling. (6) FMRP has recently been shown to be necessary for the transport of several mRNAs into dendrites, whereas neurons cultured from Fmr1 KO mice show impaired mRNA transport dynamics (Dictenberg et al., 2008). This model speculates that the trafficking population of FMRP is phosphorylated; however, future work is needed to assess whether FMRP phosphorylation may influence mRNA trafficking (From Bassell and Warren, 2008).

1.1.2 Cytoplasmic Polyadenylation Binding Protein (CPEB)

CPEB is a highly conserved, sequence-specific RNA binding protein. It binds to the cytoplasmic polyadenylation element (CPE), and modulates translational repression and mRNA localization (Mendez and Richter, 2001). After being found in Xenopus oocytes, three additional CPEB proteins containing similar RNA-binding domains were identified in mice, and thus called CPEB2–4 (Theis et al., 2003). It now appears that CPEB2–4 do not bind to the same cis-element as CPEB1 and, although they might regulate mRNA translation, they do not do so by regulating polyadenylation (Huang et al., 2006). Therefore, CPEB2–4 might represent a separate class of RNA-binding proteins. A great deal more is known about how CPEB1 regulates translation.

CPEB1 is present in many regions of the brain, including the hippocampus, the cerebellum and the cortex, where it localizes to synapses and is a component of the postsynaptic density (PSD) (Wu et al., 1998).

The CPE is bound by CPEB (Fig. 5), a highly conserved zinc finger and RNA-Recognition Motif (RRM) - type RNA-binding protein. Triggering of polyadenylation by this protein requires the kinase Eg2, an enzyme that is activated soon after *Xenopus* oocytes are exposed to progesterone (Anderson and Kedersha, 2006) and which seems to be further activated at maturation. Eg2, a member of the AURORA family of serine/threonine protein kinases, phosphorylates CPEB at serine residue 174 , an event that increases the affinity of CPEB for the cleavage and polyadenylation specificity factor (CPSF) (Mendez et al., 2000).

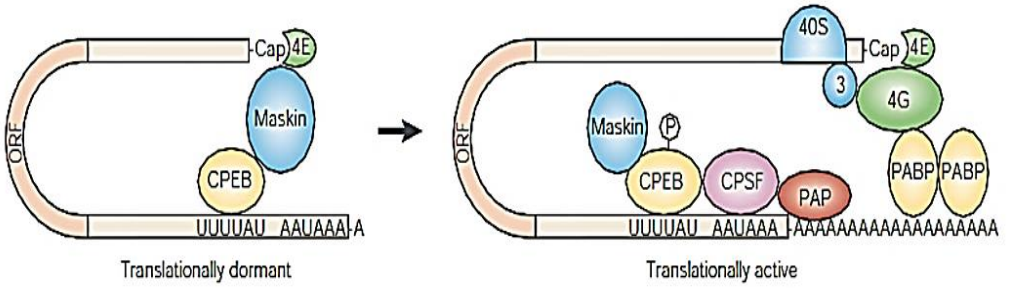

Figure 5: CPEB-mediated translational control.

In immature oocytes, messenger RNAs containing a cytoplasmic polyadenylation element (CPE) are translationally dormant (masked) and reside in a complex containing the CPE-binding protein (CPEB), maskin and eIF4E. Once maturation begins, newly phosphorylated CPEB (by the kinase Eg2) recruits the cleavage and polyadenylation specificity factor (CPSF) and poly(A) polymerase (PAP), which elongates the poly(A) tail. At a time coincident with this elongation, maskin dissociates from eIF4E. One possible cause of this maskin–eIF4E dissociation is the formation of a stable poly(A)-binding protein (PABP)–eIF4G complex, which outcompetes maskin for binding to eIF4E and thereby assembles the 48S complex. ORF, open reading frame (from Mendez and Ritcher, 2001)

The binding of CPEB1 near the end of the 3-UTR anchors a complex of proteins that include an eIF4E binding protein (Maskin), a poly(A)-polymerase (Gld2), a scaffolding protein (Symplekin) and a deadenylase (poly(A)-specific ribonuclease (PARN)). Binding of CPEB1 to the mRNA initially inhibits mRNA translation through the interaction of Maskin and eIF4E, however, CPEB1 phosphorylation leads to the dissociation of PARN from the complex and subsequent polyadenylation of tail by Gld-2 (Richter and Kim, 2006). This polyadenylation results in the dissociation of Maskin from eIF4E and the activation of translation.

CPEB1-mediated translation is activated when CPEB1 is phosphorylated at two crucial residues (Thr171 and Ser177 in mouse). In hippocampal neurons, both Aurora kinase A and αCaMKII have been implicated in the phosphorylation of this site and Aurora kinase A is thought to phosphorylate CPEB in cerebellar Purkinje neurons (Wells et al., 2007).

Furthermore, CPEB1-mediated translation can be activated following glutamate stimulation, and both NMDA-receptor- and mGluR-involvement have been described (Wells et al., 2001, Huang et al., 2002, Wells et al., 2007). Interestingly, NMDA receptor and mGluR appear to activate CPEB1-mediated translation of different mRNAs in hippocampal neurons, suggesting that CPEB1 works in concert with other regulatory mechanisms to control protein synthesis in dendrites.

1.2 Fragile X syndrome and Down's syndrome: two forms of mental retardation

Fragile X syndrome (FXS) is a prevalent form of inherited mental retardation (MR), occurring with a frequency of 1 in 4,000 males and 1 in 8,000 females. The syndrome is also characterized by developmental delay, hyperactivity, attention deficit disorder, and autistic-like behavior (Jin and Warren, 2000).

This syndrome is caused by inactivation of FMR1, a gene identified in 1991 by positional cloning and named the Fragile X Mental Retardation 1 gene (Verkerk et al., 1991). The FMR1 gene resides precisely at the cytogenetic fragile X site and was the first example of a trinucleotide repeat mutation. Within the 5'untranslated region of FMR1 there is a polymorphic CGG repeat with the most common normal length of 30 triplets. Among individuals with FXS, this repeat is found to be expanded beyond 200 repeats, typically 800 repeats, and is referred to as the full mutation. Alleles with an intermediate repeat length (55–200 repeats) are called premutations, typically found in FXS families (Bassell and Warren, 2008). Therefore, the full mutation that leads to the allele silencing and absence of the encoded protein FMRP (Fragile X Mental Retardation Protein), results in FXS.

FMRP is a protein that regulates the transport and local translation of dendritic mRNAs (see 1.1.1). For this reason, several evidences have been demonstrating that FMRP plays important roles in the adult synaptic plasticity underlying learning and memory. It also appears to be involved in axonal development, synapse formation, and the development and wiring of neuronal circuits (Gibson et al., 2008). Considering this, it is important to analyze local translation impairment in other mental retardation conditions. Down's syndrome is the spotlight of the present work.

Down's syndrome (DS) is caused by trisomy of human chromosome 21 (Hsa21) (Hassold et al., 2007), by trisomy of the long arm of Hsa21 (chr21, 21q) or, in rare cases, by partial trisomy of 21q, and by the consequent increase in expression of the triplicated genes (Siddiqui et al., 2008). This common genetic disorder affects 1 in 700-800 live births and it is the most frequent genetic cause of mental retardation (Rachidi and Lopes, 2008).

Heart defects, early-onset Alzheimer's disease (AD) and childhood leukemia are associated with the gene Hsa21 (Wiseman et al., 2009). Individuals with DS are affected by these deleterious phenotypes and by many others to a variable extent (Figure 6). To provide new insights in MR conditions, Ts65Dn and Ts1Cje mice are being valuable animal models were similar phenotypes can be expressed (Siddiqui et al., 2008). The

figure 6 shows some of the typical features of persons with segmental trisomy 21 and that are also present in Ts65Dn.

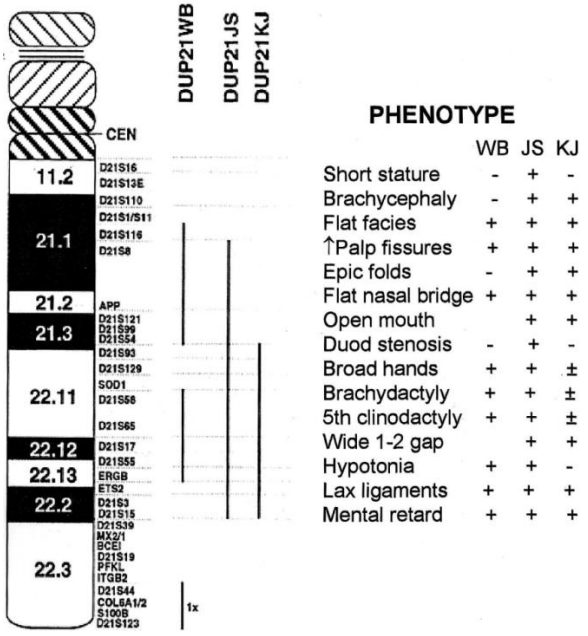

Figure 6: Components of Down's syndrome phenotype present in persons with segmental trisomy 21. The regions of trisomy in JS and KJ, indicated by the vertical bars, are quite similar to that present in the Ts65Dn mouse (From (Epstein, 2002))

The additional copy of Hsa21, in people with DS, is proposed to result in the increased expression of many of the genes encoded on this chromosome. The imbalance in expression of Hsa21 and non-Hsa21 genes is hypothesized to result in the many phenotypes that characterize DS. However, only some of the Hsa21 genes are likely to be dosage-sensitive, such that the phenotype they confer is altered by gene-copy number. Thus to understand DS, it is crucial both to understand the genomic content of Hsa21 and to evaluate how the expression levels of these genes are altered by the presence of a third copy of Hsa21 (Wiseman et al., 2009).

Brain morphology in DS at birth is primarily normal, but postnatal development slows. This results in reduced volumes of the hippocampus, cerebellum and prefrontal cortex, reduced neuronal densities in specific regions (including the hippocampus and cerebellum), and reduced dendritic branching and spine densities in the hippocampus (Nadel, 2003, Benavides-Piccione et al., 2004). Cognitive abilities in early infancy are

within the lower range of typical development, but there are decreases over the first decade. Resulting deficits in spatial learning tasks implicate the hippocampus; specific weaknesses in language skills implicate regions of the prefrontal and temporal cortices and the cerebellum; and additional deficits suggest impaired function of the prefrontal cortex (Nadel, 2003, Benavides-Piccione et al., 2004, Abbeduto et al., 2007). The postnatal appearance of many abnormalities argues for the potential for therapeutic interventions (Gardiner, 2010).

1.2.1 Dendritogenesis

Dendritic spines are the primary recipients of excitatory input in the central nervous system. They provide biochemical compartments that locally control the signaling mechanisms at individual synapses. Hippocampal spines show structural plasticity as the basis for the physiological changes in synaptic efficacy that underlie learning and memory. Spine structure is regulated by molecular mechanisms that are fine-tuned and adjusted accordingly to developmental age, level and direction of synaptic activity, specific brain region, and exact behavioral or experimental conditions. Reciprocal changes between the structure and function of spines impact both local and global integration of signals within dendrites (Bourne and Harris, 2008).

Investigations in children and adolescents with unclassified MR have confirmed reduced density and spine dysgenesis involving apical dendrites of the prefrontal cortex (Takashima et al., 1982). In fact, impairment in dendritogenesis as well as defaults in dendritic spines are common to different forms of mental retardation. In Fragile X patients, spines are longer, thinner and more abundant than in non-affected individuals (Irwin et al., 2001). In Down's syndrome, dendrites are shorter, and spines are also longer and thinner but less abundant than in normal subjects (for a review, see (Benavides-Piccione et al., 2004)). The figure 7 clearly shows the morphological impairment that exists in dendrites from retarded individuals comparing with normal ones.

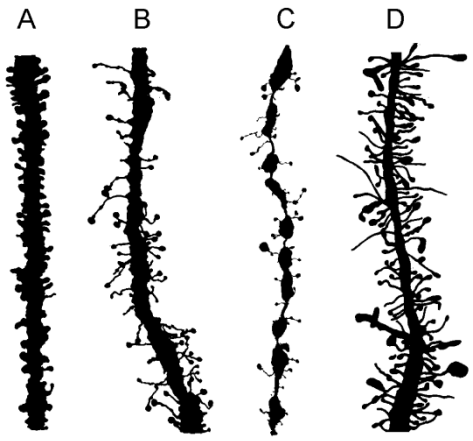

Figure 7: Camera lucida drawings of apical dendrites of pyramidal cells from human cerebral cortex. A) A dendrite from a 6-month-old infant with no history of neurological disorder has a larger number of spines. B) Dendrite from a retarded 10-month-old child shows long and tortuous spines. C) A dendrite from a 5.5-month-old child with severe neurobehavioral failure shows numerous varicosities and long, thin spines. D) A dendrite from an adult case of fragile X syndrome has a high density of elongated and enlarged spines. (Adapted from Harris, 2002 and (Rudelli et al., 1991))

1.2.2 ***Synaptic plasticity***

At the cellular level, long-lasting changes in synaptic strength, typically called synaptic plasticity, refers to the ability of neurons to alter communication with each other via synaptic connections in response to specific patterns of electrical stimulation and/or neurotrophic factors. It is generally considered to underlie long-term memory (LTM) (Malenka and Nicoll, 1997). Changes in gene expression are required to convert short term memory (STM), lasting less than 1 h, to long-term memory (LTM) in both invertebrates and vertebrates (Kandel, 2001).

The most studied forms of long-lasting synaptic plasticity in mammals, particularly rodents, are long-term potentiation (LTP) and long term depression (LTD), which refer to long-lasting increases or decreases, respectively, in synaptic strength (Malenka and Bear, 2004). Most of the work on LTP and LTD has been conducted in the hippocampus, a structure required for memory consolidation.

Synaptic plasticity is considered essential for learning and storage of new memories. Whether all synapses on a given neuron have the same ability to express long-term plasticity is not well understood. Synaptic microanatomy could affect the function of

local signalling cascades and thus differentially regulate the potential for plasticity at individual synapses (Holbro et al., 2009). Localization of mRNAs at the synapse has been proposed as a mechanism for synaptic plasticity and thus learning and memory (Klann and Dever, 2004).

In addition to mRNA localization in dendrites, there are two aspects of neuronal plasticity important for information processing: plasticity of intrinsic excitability – that is the change in ion channel properties; and synaptic plasticity - that is the change in the strength of synapses between two neurons. Although more is known about the signaling pathways underlying synaptic plasticity, many of these pathways also underlie the plasticity of intrinsic excitability (Kotaleski and Blackwell, 2010). The figure 8 summarizes the key steps on synaptic plasticity.

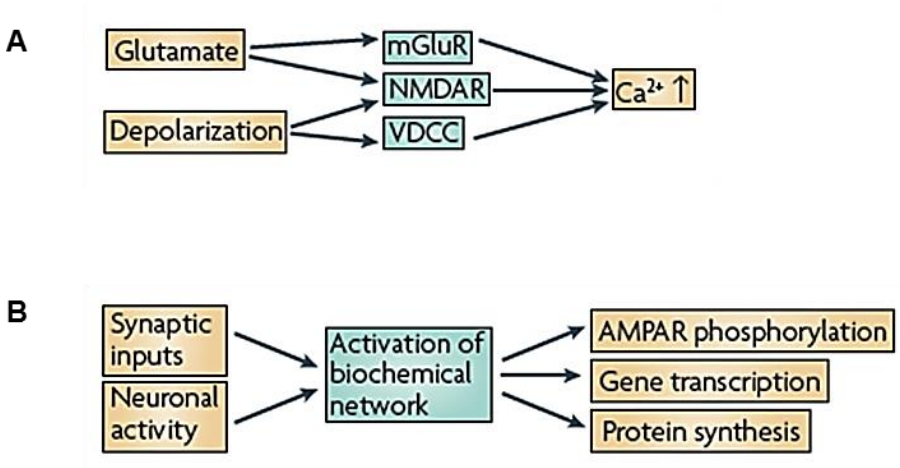

Figure 8: Succinct signaling pathways underlying synaptic plasticity.

A) Presynaptic glutamate release and depolarization of the postsynaptic neuron leads to Ca^{2+} elevation in the postsynaptic cell. Glutamate is required for activation of NMDARs (*N*-methyl-daspartate receptors) and metabotropic glutamate receptors (mGluRs), and depolarization is required for activation of NMDARs and voltage-dependent Ca^{2+} channels (VDCCs)(Perkel et al., 1993). The particular mechanism employed depends on the cell type. B) For late-phase LTP and memory storage, a combination of synaptic inputs and neuronal activity leads to AMPAR phosphorylation and membrane insertion, gene transcription and protein translation (Adapted from Kotaleski & Blackwell, 2010).

1.2.3 Down's Syndrome Cell Adhesion Molecule (DSCAM): a candidate gene

DSCAM was first identified in an effort to characterize proteins located within human chromosome band 21q22, a region known to play a critical role in Down's

Syndrome (Yamakawa et al., 1998). DSCAM promotes cation-independent homophilic intercellular adhesion (Agarwala et al., 2000), and none of the other genes in the 21q22 region are known to exhibit adhesive properties (Hattori et al., 2000). The name Down's Syndrome Cell Adhesion Molecule was chosen because of the chromosomal location, its appropriate expression in developing neural tissue, and its structure as an immunoglobulin (Ig) receptor related to other Cell Adhesion Molecules (CAMs). DSCAM proteins are one of the largest Ig superfamily CAMs discovered (220 kDa), containing 10 Ig domains and six fibronectin type III (FN) repeats, with the tenth Ig domain located between FN four and five (Fig. 9) (Schmucker and Chen, 2009).

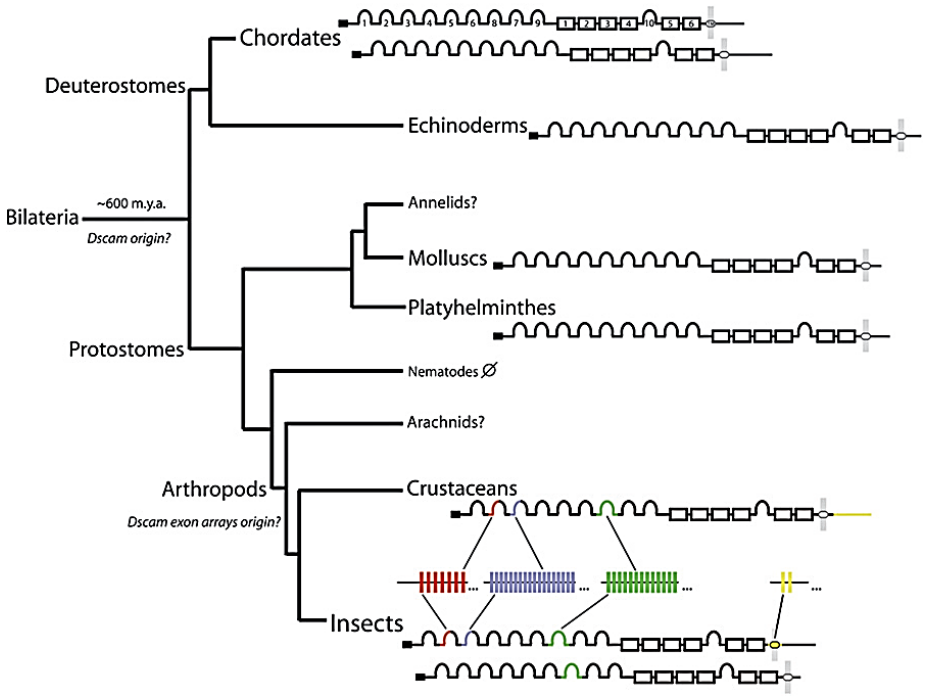

Figure 9: Phylogenetic analysis of Dscam Ig receptor.

Domain architecture of the Ig receptor Dscam is conserved over 600 million years across invertebrate and vertebrate species. Phylogenetic analysis of Dscam gene and protein structure indicates a presumptive origin of Dscam before the split of the Bilaterians. Dscam protein has nine Ig domains from N terminus, six FN domains, with a single Ig domain between FN domains four and five. The most notable difference between the arthropod and vertebrate genomic organizations is the hypervariable exon arrays in arthropods that can generate tens of thousands of Dscam isoforms. Alternative splicing of these exon array sequences (red, blue, and green) generate different sequences of the N-terminal half of Ig2 (red), the N-terminal half of Ig3 (blue), and the full Ig7 domain (green). Remarkably, alternative splicing of these specific hypervariable Ig domains is conserved between crustaceans and insects, with a common ancestor >400 million years ago. It is not known whether the annelid and arachnid genomes contain Dscam genes (?); the nematode genomes currently available do not contain Dscam (ø). (from Schmucker and Chen, 2009)

Since DSCAM identification, it has been suspected that elevated levels of DSCAM may contribute to some DS phenotypes (Yamakawa et al., 1998, Saito et al., 2000). In fact, because overexpression of DSCAM has been detected in DS patients (Saito et al., 2000), it become a strong candidate involved in mental retardation conditions.

Recently, new insights in the mouse *DSCAM* have been made. Five isoforms were isolated from neonatal (P0) and adult hippocampal mice and *DSCAM* expression in neonatal hippocampus was fourfold higher than in the adult (Alves-Sampaio et al., 2010) To characterize the regulation of *DSCAM* mRNA, functionality of the five polyadenylation hexamers was first assessed (Fig. 10). Moreover, *DSCAM* mRNA association to CPEB1 in the mouse hippocampus and dendritic local translation in response to NMDAR activity were demonstrated (Alves-Sampaio et al., 2010).

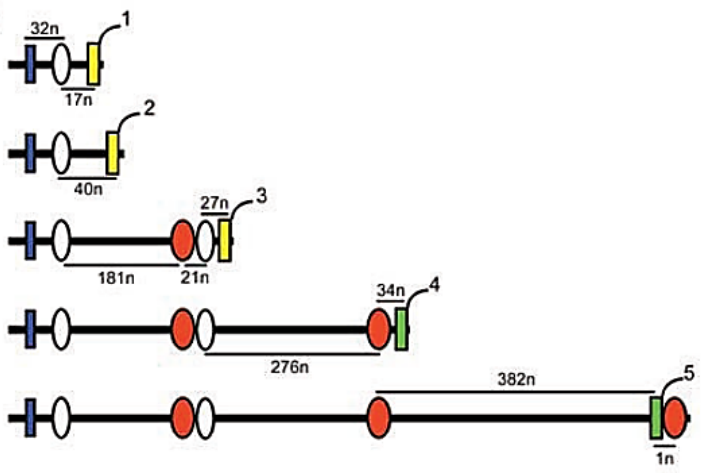

Figure 10: *DSCAM* 3'-UTR isoforms produced in mouse by alternative usage of polyadenylation hexamers 1–5.

The distances between the pairs of regulatory motifs are indicated in nucleotides (n). The Pumilio-binding element (PBE) (in blue) is shown, including the nonconsensus and consensus cytoplasmic polyadenylation elements (ncCPEs and CPEs) (in white and orange, respectively), and alternative polyadenylation hexamers (numbered from 1 to 5; AUUAAA sequence in yellow; AAUAAA sequence in green) (Adapted from Alves-Sampaio et al, 2010).

DSCAM has been shown to participate in dendritic tiling and self-avoidance in the mouse visual system (Fuerst et al., 2008, Burgess et al., 2009), two fundamental phenomena related to the formation of neural circuits. DSCAM overexpression has been shown to inhibit dendritic arborization of mouse hippocampal neurons (Alves-Sampaio et al., 2010). A role of DSCAM in adult hippocampal neurogenesis has also been suggested

(Yamashima et al., 2007). DSCAM is strongly expressed during brain development, and although it is downregulated in the adult, its expression persists in brain areas with high levels of synaptic plasticity, including the cortex, hippocampus, and cerebellum (Agarwala et al., 2001, Barlow et al., 2001). Nonetheless, the function of DSCAM in the adult brain remains unknown.

1.2.4 Dendritic targeting elements (DTEs) and local translation reporters

As mentioned before, in neurons, activity-dependent mRNA targeting establishes certain forms of synaptic plasticity through new local protein synthesis in dendrites, and it is critical for proper responses to extracellular stimuli (Aakalu et al., 2001). Thus, transport of mRNAs to dendrites is a prerequisite for local protein synthesis. Recognition of cis-acting elements in mRNAs by trans-acting RNA binding proteins is thought to underlie selective mRNA targeting. While several cis-acting dendritic targeting elements (DTEs) have been identified in dendritic mRNAs (Blichenberg et al., 1999, Kobayashi et al., 2005), only a few trans-acting RNA binding proteins are known (Huang et al., 2003).

The Cytoplasmic Polyadenylation Element (CPE), a cis element in the 3'UTRs of specific dendritic mRNAs, promotes cytoplasmic polyadenylation-induced translation in response to synaptic stimulation. It has been demonstrated that the CPE and its binding protein CPEB facilitate mRNA transport to dendrites (Huang et al., 2003). *DSCAM* isoforms analysed in this work (isoforms 1, 3, 4 and 5) are originated by alternative polyadenylation and bear different combinations of regulatory CPE motifs (Fig. 10). Thus, dendritic local translation of some of these isoforms is regulated by CPEB protein (Alves-Sampaio et al., 2010).

Fluorescent protein-based translation reporters allow the dynamically visualization of local synthesis of proteins in neuronal processes. The first such tools developed used a diffusion limited fluorescent translation reporter in which a region encoding a destabilized, myristoylated green fluorescent protein (GFP) is flanked by the 5' and 3' untranslated regions (UTRs) from αCaMKII mRNA (Aakalu et al., 2001), an mRNA known to be dendritically localized. The half-life of this destabilized GFP is >90 min, and the myristoylation tag has been shown to severely inhibit the free diffusion of the reporter once translated (Aakalu et al., 2001). This translation reporter has been used to examine both activity-dependent (Sutton et al., 2004) and neuromodulatory control (Aakalu et al., 2001, Smith et al., 2005) of dendritic protein synthesis in hippocampal neurons.

One of the major improvements in this class of translation reporter has come from replacing a generic fluorescent protein with either photoconvertible fluorescent proteins (Kaede or Dendra) or epitope tags that bind spectrally distinct fluorescent dyes with high affinity (e.g., FlAsH/ReAsH). These modifications make it possible to distinguish newly synthesized reporter from preexisting fluorescent signal. Also, they allow for a more precise "dating" of new reporter signal without the need for photobleaching existing signal. These newer reporter systems have been used to examine local synthesis of sensorin at Aplysia synapses (Wang et al., 2009) and local dendritic synthesis of AMPA receptor subunits GluA1 and GluA2 (Ju et al., 2004) as well as Kv1.1 voltage-gated potassium channels (Raab-Graham et al., 2006).

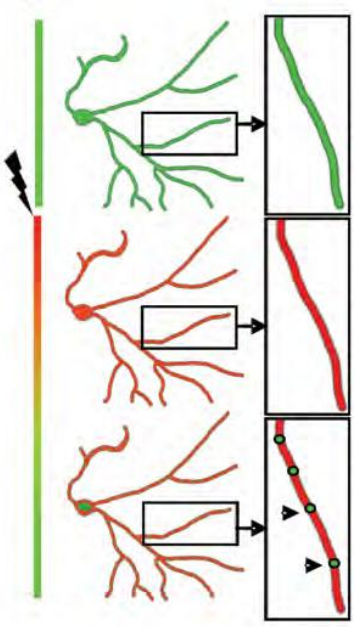

Figure 11: Local translation assay using photoconvertible protein Kaede.

Schematic of local translation assay using the photoconvertible protein Kaede. Left side shows neuron with boxed dendrites; right side shows enlargement. Green puncta indicate local translation "hot spots." Kaede initially appears green, but with UV exposure, is converted to red. New protein synthesis is monitored by the appearance of new green protein over time (arrowheads) (Adapted from Raab-Graham et al 2006).

1.3 Aim of this work

Local translation of specific mRNAs at the synapse has been proposed as one of the mechanisms responsible for plasticity and thus learning and memory. FMRP and CPEB are two important recognized proteins involved in mRNA translation in dendrites. FMRP loss of function leads to Fragile X mental retardation, in which learning and memory are impaired. This highlights the importance of local translation for cognition. DSCAM belongs to the largest group of the immunoglobulin (Ig) related cell adhesion molecules and is involved in a number of important biological processes. This gene is located in the Down's Syndrome Critical Region (DSCR), in HSA21. Interestingly, *DSCAM* is a putative FMRP-target gene (Brown et al., 2001) and its local translation is regulated by CPEB in hippocampal neurons (Alves-Sampaio et al., 2010). Thus, altered local translation of *DSCAM* could be responsible, at least in part, of some of the neuronal phenotypes associated to DS.

In previous work, DSCAM isoforms 1, 3, 4, and 5 were amplified from mouse hippocampal cDNAs. Some of this isoforms were shown to be under the control of CPEB protein in *Xenopus* oocytes. However the regulation of dendritic local translation of *DSCAM* isoforms in hippocampal neurons is unknown. To provide new insights in the role of *DSCAM* isoforms, and most specifically, in the specific regulation of each DSCAM isoform, a photoconvertible reporter protein was chosen for visualizing and localizing the expression of those isoforms in transfected hippocampal neurons.

The objectives of this study were:

- To modify the original Kaede plasmid, in order to use it as a reporter for local translation.

- To visualize the expression of Kaede-DSCAM-isoform constructions in hippocampal neuron cultures.

2. Material and Methods

2.1 Kaede plasmid (pKaede) modification

pKaede – MC1 (Amalgaam, MBL, Japan) plasmid obtained at the dry form (20µg), was resuspended in 20µl of distilled sterile water. To perform the vector linearization, 5µg of pKaede were digested with 1µl of the restriction enzyme, BamHI (10U) purchased from TaKaRa BIOTECH Co. (Japan). After 4 hours at 37^0C, succeeded procedure was confirmed by electrophoresis of 1µl of digestion product through a 0.8% agarose gel. The subsequent 19µl of digestion product was dephosphorylated with 1µl of alkaline phosphatase (20U/µl) following manufacturer´s procedure. The mixture was incubated for 30m at 37^oC. Electrophoretic separation was performed to isolate the linearized and dephosphorylated vector from a 0.8% agarose gel. DNA was extracted from the agarose using the QIAEX II Agarose Gel extraction Protocol, according to the manufacturer's instructions.

To insert a stop codon at the end of Kaede protein in pKaede-MC1 (for generating pKaede-3'UTR), two complementary oligos were designed that also included NheI and EcoRV restriction sites. These oligos named Stop-BamHI-fw and STOP-BamHI-rv were annealed using the precise concentrations and volumes mentioned in the table below. The mixture (100µl) was introduced in a bath (glass cup with water at 100^0C) and maintained at room temperature until it decreases to 37^0C.

Table 1: STOP-BamHI annealing mixture reaction composition.

Oligos/ Buffer	**Concentration** (µM, mM)	**Volume** (µl)
STOP-BamHI-fw, 5´[Phos] GATCTTAATGATATCG	10 µM	10µl
STOP-BamHI-rv, 5´[Phos] GGGATCCGATATCATTAA	10 µM	10µl
Buffer Tris$MgCl_2$: Tris $MgCl_2$	 62,5 mM, pH7,6 12,5 mM	80µl

When annealed, these oligos generate BamHI-compatible ends, and this fragment was ligated to the pKaede vector (linearized with BamHI and dephosphorylated). We used 3µl of pKaede, 1µl of STOP-BamHI reaction product, 5 µl of Rapid Buffer and 1µl of T4

DNA ligase 3U/µl (Promega). After 1h of incubation at room temperature, the final volume of ligation reaction (10 µl) was used to transform 50µl of Competent Cells (Subcloning Efficiency™ DH5α™, Invitrogen). The transformation method used was heat-shock: incubation in ice for 30 min, incubation at 37^{0}C for 20 sec followed by a 2 min incubation in ice. Then, 400µl of LB medium was added and this new mix was incubated for 1h at 37^{0}C. To concentrate the transformation mix, a centrifugation at 14.000 rpm for 1 min was performed; 300µl of supernatant removed and the remaining 100µl of the pellet was spread in plates with the selective culture medium, LB with Kanamycin 50 µg/ml.

After over-night incubation at 37^{0}C, six selected colonies were inoculated in 3,5ml of LB with Kanamycin 25µg/ml. DNA of each presumable transformed colony was extracted and purified 24 hours later through the Pure Link Quick Plasmid Miniprep kit (Invitrogen), accordingly to manufacturer's instructions. Inserted STOP oligos in pKaede were confirmed by restriction with EcoRV and the transformed plasmid with the correct orientation was selected by sequencing.

To confirm the presence of NheI restriction site and perform the vector linearization for the subsequent modifications, 5µg of pKaede-3'UTR were digested with 1µl of the restriction enzyme NheI (10U) purchased from TaKaRa BIOTECH Co. (Japan). After 4 hours at 37^{0}C, succeeded procedure was confirmed by electrophoresis of 1µl of digestion product through a 0.8% agarose gel. The subsequent 19µl of digestion product was dephosphorylated with 1µl of alkaline phosphatase (20U/µl) following manufacturer´s procedure. The mixture was incubated for 30m at 37^{0}C. Electrophoretic separation was performed to isolate the linearized and dephosphorylated vector from a 0.8% agarose gel. DNA was extracted from the agarose using the QIAEX II Agarose Gel extraction Protocol, according to the manufacturer's instructions.

To insert a myristoylation signal at the 5'UTR of Kaede protein in pKaede-3'UTR (for generating p5'UTR-myrKAEDE-3'UTR), two complementary oligos were designed. These oligos named 5-UTR-myr-fw and 5-UTR-myr-rv were annealed using the precise concentrations and volumes mentioned in the table 3. The mixture (100µl) was introduced in a bath (glass cup with water at 100^{0}C) and maintained at room temperature until it decreases to 37^{0}C.

When annealed, these oligos generate NheI-compatible ends and contain EcoRV restriction site, a Kozak sequence and a myristoylation signal. This fragment was ligated to the 5'UTR of pKaede-3'UTR (linearized with NheI and dephosphorylated). We used 3µl of pKaede-3'UTR, 1µl of 5-UTR-myr reaction product, 5 µl of Rapid Buffer and 1µl of T4 DNA ligase 3U/µl (Promega). After 1h of incubation at room temperature, the final volume

of ligation reaction (10 µl) was used to transform 50µl of Competent Cells (Subcloning Efficiency™ DH5α™, Invitrogen). The transformation method used here was the same described previously. DNA of each presumable transformed colony was extracted and purified 24 hours later through the Pure Link Quick Plasmid Miniprep kit (Invitrogen), accordingly to manufacturer's instructions. Inserted myristoylation signal in pKaede-3'UTR was analysed by restriction with EcoRV and the six hypothetical p5'UTR-myrKAEDE-3'UTR plasmids were sequenced.

Table 2: 5-UTR-myr annealing mixture reaction composition.

Oligos/ Buffer	**Concentration** (µM, mM)	**Volume** (µl)
5-UTR-myr-fw, 5´[Phos]CTAGGCTAGCGATATCGCCACCATGG GCACGGTGCTGTCCCTATCTCCCAGCC	10 µM	10µl
5-UTR-myr-rv, 5´[Phos]CTAGGGCTGGGAGATAGGGACAGCAC CGTGCCCATGGTGGCGATATCGCTAGC	10 µM	10µl
Buffer Tris$MgCl_2$: Tris $MgCl_2$	 62,5 mM, pH7,6 12,5 mM	80µl

2.2 Cloning of DSCAM isoforms in pKaede

Sequences corresponding to the 3'-UTR of the *DSCAM* isoforms 1, 3, 4, and 5 were originally amplified from mouse hippocampal cDNA by PCR and cloned downstream the Firefly luciferase coding region of the pLucCassette vector (Alves-Sampaio et al., 2010). These vectors were used in the present work. The *E.coli* clones containing *DSCAM* isoforms 1, 3, 4 and 5 (*DSCAM*-isof1, *DSCAM*-isof3, *DSCAM*-isof4, *DSCAM*-isof5) stored at -80^{0}C, were cultured in 100ml of LB 50µg/ml ampicilin. Cultures were incubated overnight at 37^{0}C, 200rpm. After this period, DNA was isolated using the Pure YieldTM Plasmid Midiprep System (Invitrogen). The yield of total DNA was determined by measuring the absorbance (260-280 nm; 260-230 nm) using a NanoDrop ND-1000 spectrophotometer. DNA fragments containing the 3'UTR region of the corresponding *DSCAM* isoform were obtained by doubled digestion, with BamHI and BglII. Whereas both digestions require 4 hours of incubation at 37^{0}C, these restriction enzymes have different reaction buffers. For this reason, it was necessary to wash the first digestion product with the Sure Clean Plus kit (Bioline) before the second digestion. This is one of the several critical steps of the procedure were DNA can be lost. So, to obtain enough quantity of each DNA fragment, 15 µg of total DNA was used at the beginning of the procedure (the first digestion). After the second digestion with BglII a preparative electrophoresis was made to separate DNA fragments. To avoid contaminations, all the electrophoretic material was washed with 10% SDS and the TAE (1X) renewed in the tank. To purify the isolated fragment from the 0,8% agarose gel, the slice of gel containing DNA was dissected and the QIAEX II Agarose Gel extraction kit was used, according to the manufacturer's instructions.

The four different inserts isolated and purified: *DSCAM*-isof1, *DSCAM*-isof3, *DSCAM*-isof4, *DSCAM*-isof5 were then prepared for ligation with the Kaede plasmid (linearized with BamHI and dephosphorylated). Ligation of the vector with the four different isoforms was made using the same method described in 2.1. We used 3µl of pKaede, 1µl of the insert, 5 µl of Rapid Buffer and 1µl of T4 DNA ligase 3U/µl. After 1h of incubation at room temperature, the final volume of ligation reaction (10 µl) was used to transform competent cells. For transformation, different competent cells were used. To clone *DSCAM*-isof1, *DSCAM*-isof3, *DSCAM*-isof5, 50 µl of DH5α^{TM} (Subcloning Efficiency^{TM} Competent Cells, Invitrogen) was used. In the case of the plasmid containing *DSCAM*-isof4, we had to use Chemically Competent E.coli (One Shot® Mach1 ^{TM} -T1^R,

Invitrogen). The transformation method used was heat-shock: incubation in ice for 30 min, incubation at 37^0C for 20 sec followed by a 2 min incubation in ice. Then, 400µl of LB medium was added to each tube and this new mix was incubated for 1h at 37^0C. To concentrate the transformation mix, a centrifugation at 14.000 rpm for 1 min was done, 300µl of supernatant removed and the remaining 100µl of the corresponding pellet was spread in a plate with the selective culture medium (LB with 50 µg/ml Kanamycin). After over-night incubation at 37^0C, four colonies from each plate were inoculated in 3,5ml of LB with 25µg/ml of Kanamycin. DNA of each presumable transformed colony was extracted and purified 24 hours later through the Pure Link Quick Plasmid Miniprep kit (Invitrogen), according to manufacturer's instructions. Inserted *DSCAM* isoforms in pKaede were confirmed by restriction with EcoRI and the transformed plasmids with the sense and anti-sense orientation were identified and selected after sequencing.

2.3 Hippocampal neuron cultures

Animals were maintained, handled, and sacrificed in accordance with national and international laws and policies, and all protocols were approved by the University of Seville Animal Care and Use Committee.

The hippocampus from postnatal day 0 (P0) wild-type mouse littermates was dissected out in HBSS medium (Invitrogen) and mechanically dissociated after trypsin treatment (0.2% trypsin for 10 min at 37°C) in DB1 culture medium (DMEM high glucose with L-glutamine, without sodium pyruvate; 10% fetal bovine serum; Glutamax; 08% glucose; penicillin/strep-tomycin).

Cells in suspension were counted using a haemocytometer (Neubauer, Poly-labo; depth = 0.100mm, square surface on the grid = 0.0025 cm^2) under an inverted phase contrast microscope (Zeiss, Germany).

The cells (80.000 cells/well) were seeded on poly-L-lysine-treated coverslips (0.5 mg/ml) and cultured in Neurobasal A medium (Neurobasal A; B27 supplement; Glutamax; penicillin/streptomycin), in 6-well plates. After 48 h in culture, 0.3 mM 5-fluoro-2-deoxyuridine (Sigma-Aldrich) and 0.8 mM uridine (Sigma-Aldrich) were added to the culture medium to inhibit glial growth.

2.4 Cell transfection

By definition, transfection is the introduction of a foreign DNA molecule into a eukaryotic cell and the subsequent expression of one or more genes in the transfected cell (Alberts et al., 1994). Many different chemical agents that facilitate transfection are commercially available.

Two different methods were used in this work: the liposome method and the calcium phosphate coprecipitation method. In the liposome method, Lipofectamine 2000 (Invitrogen) was used, following the manufacturer's instructions, for transfection of day 7 in vitro (DIV7) hippocampal neurons. In this method, positive charged liposomes bind to the negatively charged phosphates of the DNA molecules to form a complex with a surplus of positive charge. This positive charge is attracted to the negative charge of the sialic acid residues on the surface of the cell. Then the DNA-liposome complex is taken up by endocytosis (Farhood et al., 1994). Due to high efficiency, simplicity and versatility, this method was used to test the expression capacity of the reporter pKaede (CoralHue®; Amalgaam) compared with the constructed Kaede-3'UTR plasmid. A total of 4 µg of each plasmid was transfected per well. Effects on dendrite arborization were analyzed 2 days after transfection. Two independent experiments, using different batches of neurons, were performed (three transfections per experiment and plasmid).

Established in the 1970's by Graham and van der Eb (Graham and Vandereb, 1973), the second method involves the formation of a calcium phosphate/DNA precipitate that sediments, attaches to the cells and is taken up by endocytosis (Chalberg et al., 2001). For transfection of neurons with the four constructions of mouse DSCAM along with photoconvertible fluorescent protein Kaede (Kaede-*DSCAM*-isof plasmids) calcium phosphate method was chosen for being less toxic to cells.

A total of 14µg/well of DNA of each DSCAM construction per well was used for transfection with this method. The first step consists in preparing the transfection mix, the calcium solution (2.5 M $CaCl_2$ (SigmaC3881), 10µl/well) and DNA (14 µg/well, 90 µl/well) in individual 1.5 ml tubes (one per well). Then, the precipitate is formed by adding 2xBES (N, N-bis(2-hydroxyethyl)-2-aminoethanesulfonic acid) - Buffered Solution (2xBBS) dropwise using a vortex (Agimatic S) simultaneously for mixing the solution in the tube. This solution is incubated for 45 min in the dark. During this period, 1.8 ml of Neurobasal culture medium (GIBCO) is put in 15ml Falcon tubes and incubated at 37°C for temperature and pH adjustments. After this period, the mixture of DNA-$CaCl_2$-BBS is

added to in prewarmed culture medium and transferred to the wells. The cover slips containing the DIV7 hippocampal neurons were transferred to these new plates containing the transfection mix and incubated for 1h30m at 37^0C. The plates with the original culture medium were stored at 37^0C. After this period, the transfection mix is removed and the cover slips are gently washed 3 times with Hank's Balanced Salt Solution (HBSS) without Ca^{2+} and without Mg^{2+} (GIBCO). Finally, cover slips with the transfected neurons were put back in the original plates. After 2-4 days of incubation, cells were observed in an Olympus confocal microscope.

2.5 Confocal analysis of transfected neurons

Image processing was performed in a Confocal Laser Scanning Biological Microscope (Olympus). Hippocampal neurons cultured in 25 mm diameter coverslips and transfected at DIV7, were located on a quartz slide and visualized *in vivo.* The images were captured using two channels (red and green) and a staking of several slices were taken per image. The table 2 and the figure 12 show the precise excitation values used for Kaede fluorescence emission detection.

Table 3: Excitation light used to elicit Kaede green and red fluorescence.

	Excit./Emiss.Maxima (nm)	Extinction Coefficient ($M^{-1}cm^{-1}$)	Fluorescence Quantum Yield	pH sensitivity
Green	508/518	98,800 (508 nm)	0.88	pKa=5.6
Red	572/580	60,400 (572 nm)	0.33	pKa=5.6

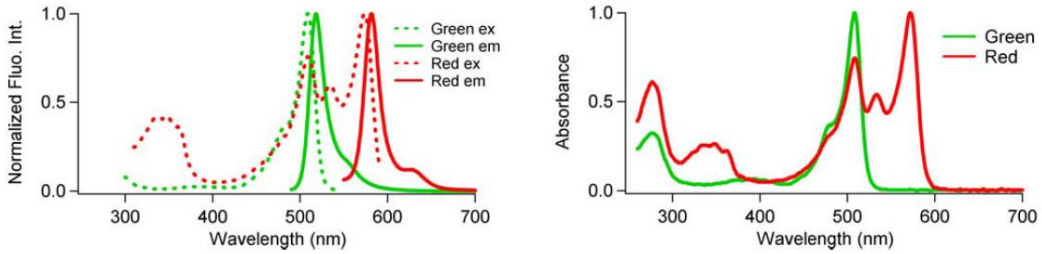

Figure 12: Spectra of green and red states of Kaede protein.

3. Results

3.1 Kaede plasmid modification

Kaede protein is a fluorescent protein from a stony coral, *Trachyphyllia geoffroyi*, and it was cloned by Ando et al (2002). Kaede protein emits green, yellow and red light and includes a tripeptide, His-Tyr-Gly, that acts as a green chromophore that can be converted to red. The red fluorescence is comparable in intensity to the green fluorescence and is stable under usual aerobic conditions. Experiments proved that the green-red conversion is highly sensitive to irradiation with UV or violet light (350–400 nm), which excites the protonated form of the chromophore. The excitation lights used to elicit red and green fluorescence do not induce photoconversion (Ando et al., 2002). The pKaede-MC1 plasmid map used in this work is shown in the figure 13.

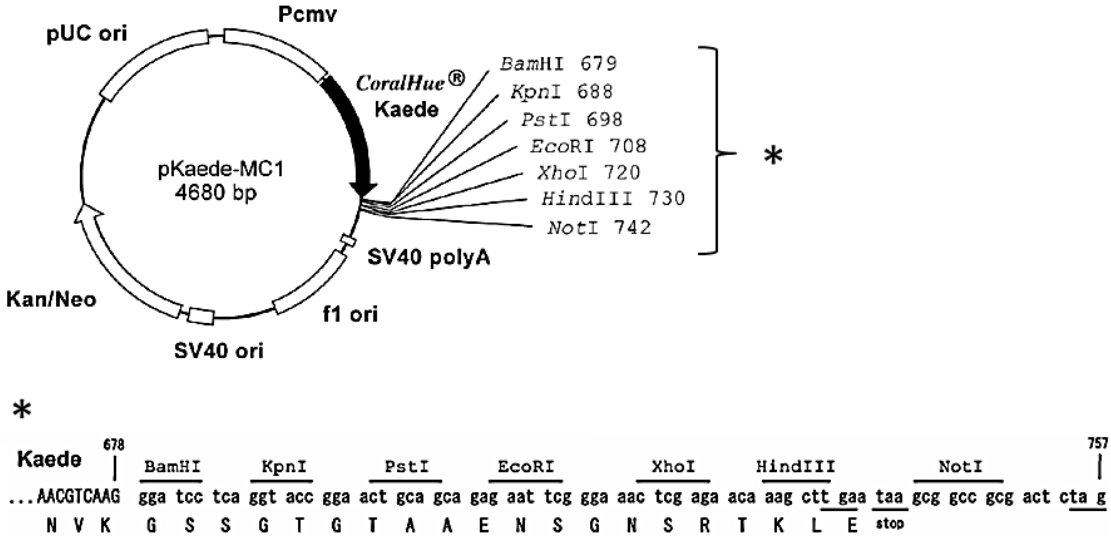

Figure 13: Map of the plasmid pKaede MC1.

Some restriction sites are shown and nucleotide sequence of each one is highligted by an asterisk (*). Kan/ Neo is the Kanamycin /Neomycin resistance gene for plasmid selection in *E.coli*. The nucleotide sequence of pKaede-MC1 is deposited in GenBank under the accession number AB085641.

The comercial pKaede-MC1 plasmid is originally designed for expressing Kaede-fusion proteins in eukaryotic cells. Thus, it lacks stop codons at the end of the Kaede coding sequence. To generate an improved version of the this pasmid to be used as a

local translation reporter, first step consisted in introducing a stop codon at the BamHI restrition site.

In order to perform the plasmid linearization, the restrition enzime BamHI was used. As expected, only one fragment between 4,000 bp and 5,000 bp (~4,680 bp) was observed in the agarose gel after electrophoresis (Fig. 14).

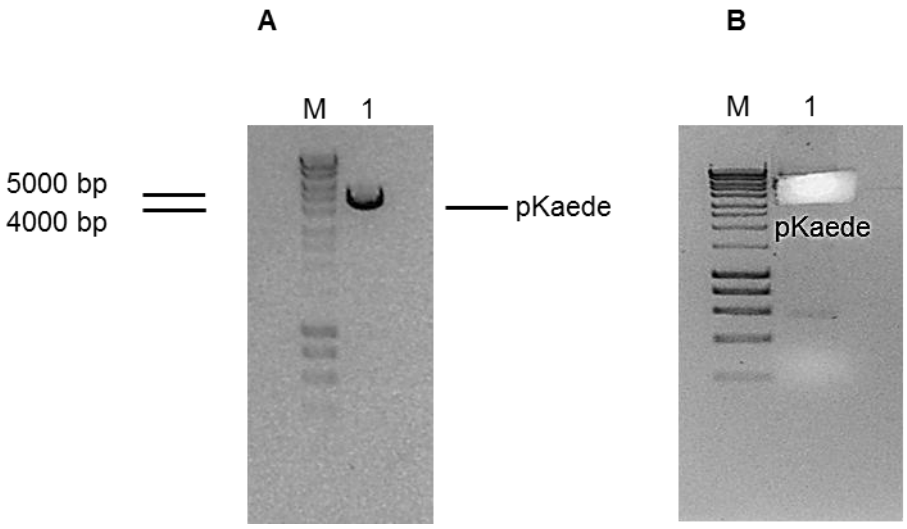

Figure 14: Restriction of pKaede plasmid with BamHI.

A) After restriction with BamHI, an aliquot (1µl of dephosphorylated product) was visualized after electrophoresis. B) Preparative gel electrophoresis of approximately 5µg of linearized and dephosphorylated pKaede plasmid after extraction of DNA for subsequent purification.

To insert a stop codon at the end of Kaede protein in pKaede-MC1, two complementary oligos named STOP-BamHI- fw and STOP-BamHI-rv were designed. These oligos were annealed and ligated to the BamHI-digested pKaede-MC1 plasmid. After *E. coli* transformation, six colonies were selected and analyzed. Insertion of the STOP-BamHI fragment was expected to originate new NheI and EcoRV sites (included in the STOP-BamHI oligos). Thus, to confirm oligo insertion, a restriction analysis using EcoRV was performed. The original pKaede sequence contains two EcoRV sites. As observed in figure 15, three main fragments of the expected size were obtained; one less-intense band probably corresponding to a non-digested, supercoiled form of the corresponding plasmid was also appreciable, migrating at a position equivalent to 600 bp.

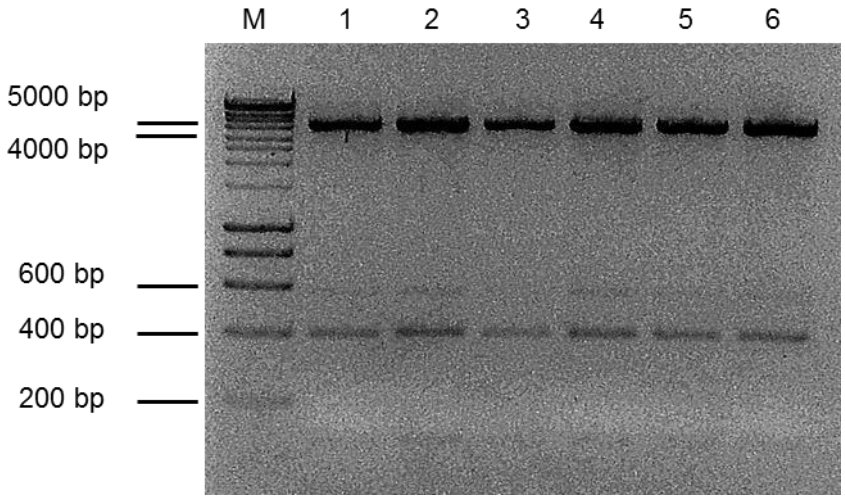

Figure 15: EcoRV restriction analysis of pKaede plasmid containing the STOP-BamHI fragment.
Obtained bands between 5 kb and 4 kb, about 400 bp and 100 bp corresponded to the expected sizes. The less-intense band (600 bp) probably corresponded to a non-digested, supercoiled form.

All the six hypothetical pKaede-3'UTR were sequenced. This confirmed the correct insertion of the STOP-BamHI oligos, the presence of the EcoRV restrition site and the regeneration of the BamHI site in one of the transformed colony (Fig. 16).

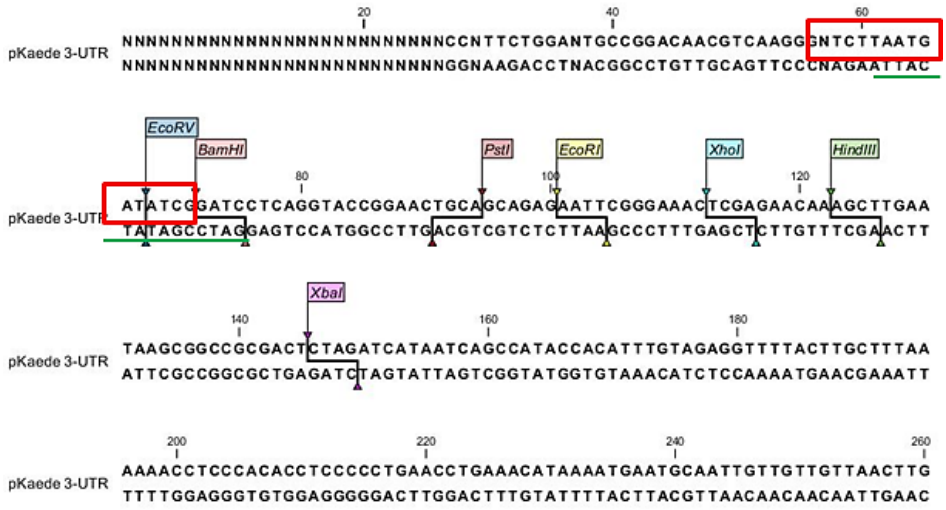

Figure 16: Correct insertion of STOP-BamHI oligo in pKaede (pKaede-3'UTR).
The red box and the green line highlight respectively, the STOP-BamHI-fw and the STOP-BamHI-rv annealed oligos. The correct insertion originated the EcoRV restriction site and the regeneration of BamHI restriction site. This graph was obtained using the free version of CLC Sequence Viewer program.

The introduction of a stop codon at the BamHI restriction site of pKaede MC1 plasmid, resulted in the pKaede-3'UTR. Besides the EcoRV restriction analysis and the plasmid sequencing have confirmed the correct insertion of STOP-BamHI oligos in the BamHI-digested pKaede-MC1, the presence of a unique restriction site upstream Kaede coding sequence was also determinant to continue the pKaede MC1 modification. This modification consisted in introducing a myristoylation signal upstream Kaede protein, in order to limit the diffusional rate of the protein.

NheI restriction analysis confirmed the presence of only one NheI restriction site which allowed us to perform pKaede-3'UTR linearization (Fig. 17).

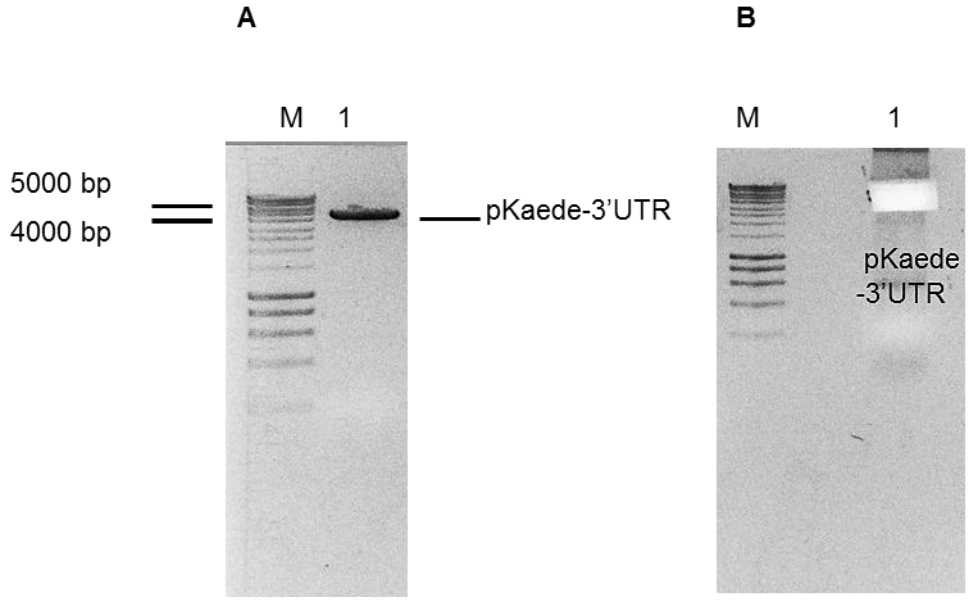

Figure 17: Restrition of pKaede-3'UTR plasmid with NheI.

A) After restriction with NheI, an aliquot (1µl of dephosphorylated product) was visualized after electrophoresis. B) Preparative gel electrophoresis of approximately 5µg of linearized and dephosphorylated pKaede-3'UTR plasmid after extraction of DNA for subsequent purification.

The linearized and dephosphorylated form of pKaede-3'UTR with NheI compatible ends was used for ligation with the annealed 5-UTR-myr-fw and 5-UTR-myr-rv designed oligos (Table 2). After *E. coli* transformation, six colonies were selected and analyzed (Figure 18). Insertion of annealed 5-UTR-myr oligos were expected to originate an extra EcoRV site, a Kozak sequence and a myristoylation signal in frame with Kaede protein. To confirm oligo insertion, an EcoRV restriction analysis was performed. As can be observed in the figure 18, in four of the transformed colonies (numbers 1, 2, 3 and 5) four

main fragments were observed (in addition to the non-digested 600bp-migrating form), suggesting that the 5'UTR-myr oligos were successfully inserted. In the other two colonies (numbers 4 and 6) a similar pattern to that of the pKaede-3'UTR plasmid was obtained, indicating that in this case the oligo containing the myristoyltion signal was not inserted.

All the four hypothetical p5'UTR-myrKAEDE-3'UTR were sequenced but the 5-UTR-myr oligos were inserted in the antisense orientation in all cases.

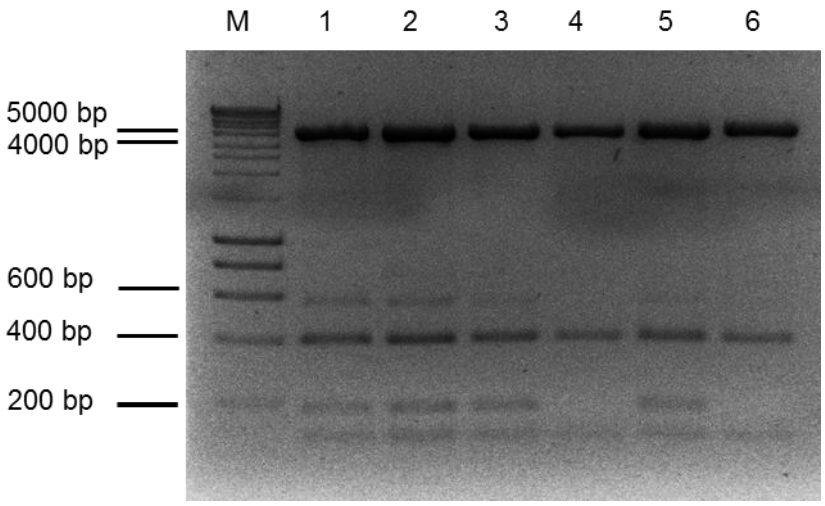

Figure 18: EcoRV restriction analysis of pKaede-3'UTR plasmid for testing 5'UTR-myr fragment insertion.

In the transformed colonies 1, 2, 3 and 5 four fragments are observed. In the other two colonies (4 and 6) three fragments are observed.

3.2 Generation of DSCAM local translation reporters based on Kaede plasmid

3'UTR from *DSCAM* isoforms 1, 3, 4 and 5 were obtained by double digestion with BamHI and BglII of the corresponding pLucCassette plasmids (see Material and Methods 2.2). The isolated *DSCAM* 3'UTR isoforms obtained using these two enzymes generate DNA fragments with BamHI compatible ends.

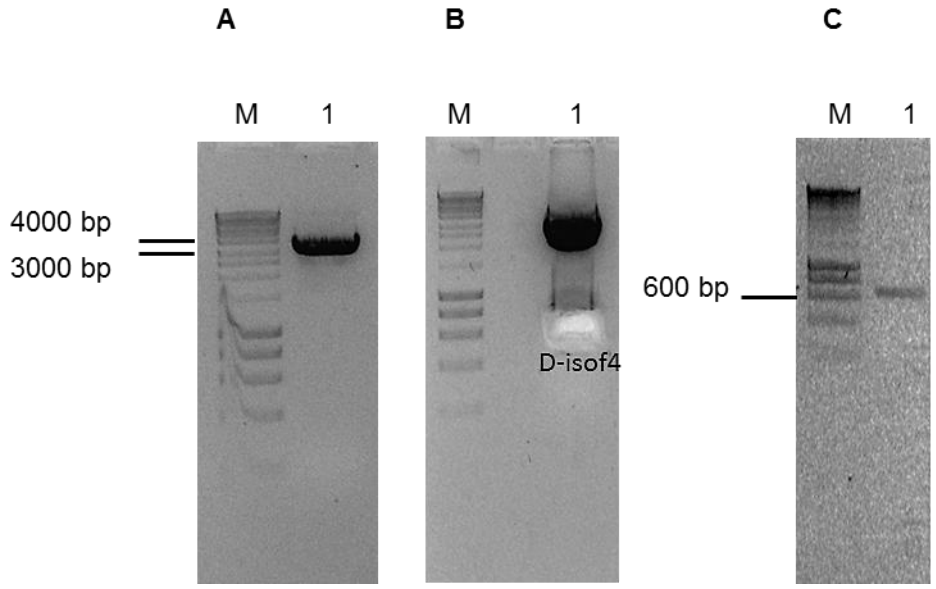

Figure 19: Isolation of DSCAM 3'UTR isoforms from the corresponding pLucCassette vector.
Restriction analysis performed to obtain the *DSCAM* isoforms 1, 3, 4 and 5 (*DSCAM*-isof1, *DSCAM*-isof3, *DSCAM*-isof4, *DSCAM*-isof5). A) The first restriction enzyme BamHI linearizes the plasmid. B) After the second digestion (BglII) two fragments are obtained. The fragment between 3000bp and 4000bp corresponds to the vector. The other one (extracted in the picture shown in panel B) corresponds to *DSCAM*-isof4 in this particular example. The succeeded purification of this fragment with about 600bp is confirmed as observed in panel C.

The original pKaede plasmid linearized with BamHI and dephosphorylated was used for direct cloning of *DSCAM* 3'UTR isoforms. The modified pKaede, pKaede-3'UTR was not used to conduct these constructions because the desired modifications of the

plasmid (p5'UTR-myrKAEDE-3'UTR) were not achieved in time. As the matter of fact, at the beginning of the experiments we also wanted to know if the original plasmid Kaede together with the *DSCAM* isoforms were expressed in hippocampal neuron cultures. So, Kaede plasmid modification and cloning of *DSCAM* 3'UTR isoforms in the original Kaede plasmid were performed at the same time.

To obtain pKaede-*DSCAM*-isoforms several attempts were made. The figure 20 shows the corresponding inserts separated from pKaede after restriction analysis with EcoRI.

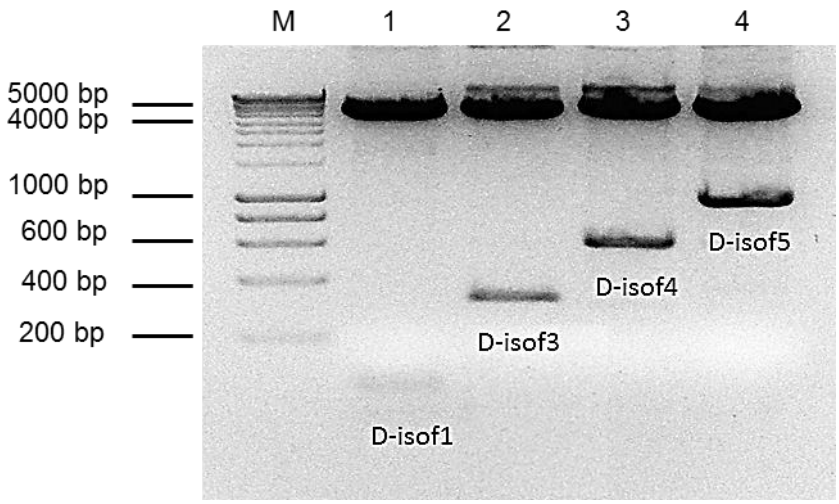

Figure 20: Constructions of pKaede with the *DSCAM* isoforms 1, 3, 4, 5 confirmed by restriction with EcoRI.

The bands located between 5kb and 4kb correspond to pKaede vector. The other bands are identified in the figure by the name of the corresponding *DSCAM* isoform ("D-isof" is an abbreviation of "*DSCAM*-isoform").

The correct (i.e., *sense*) orientation of these constructions was confirmed by sequencing (see Appendix), comparing the sequences with the original *DSCAM* isoforms 1, 3, 4 and 5 (Fig. 21).

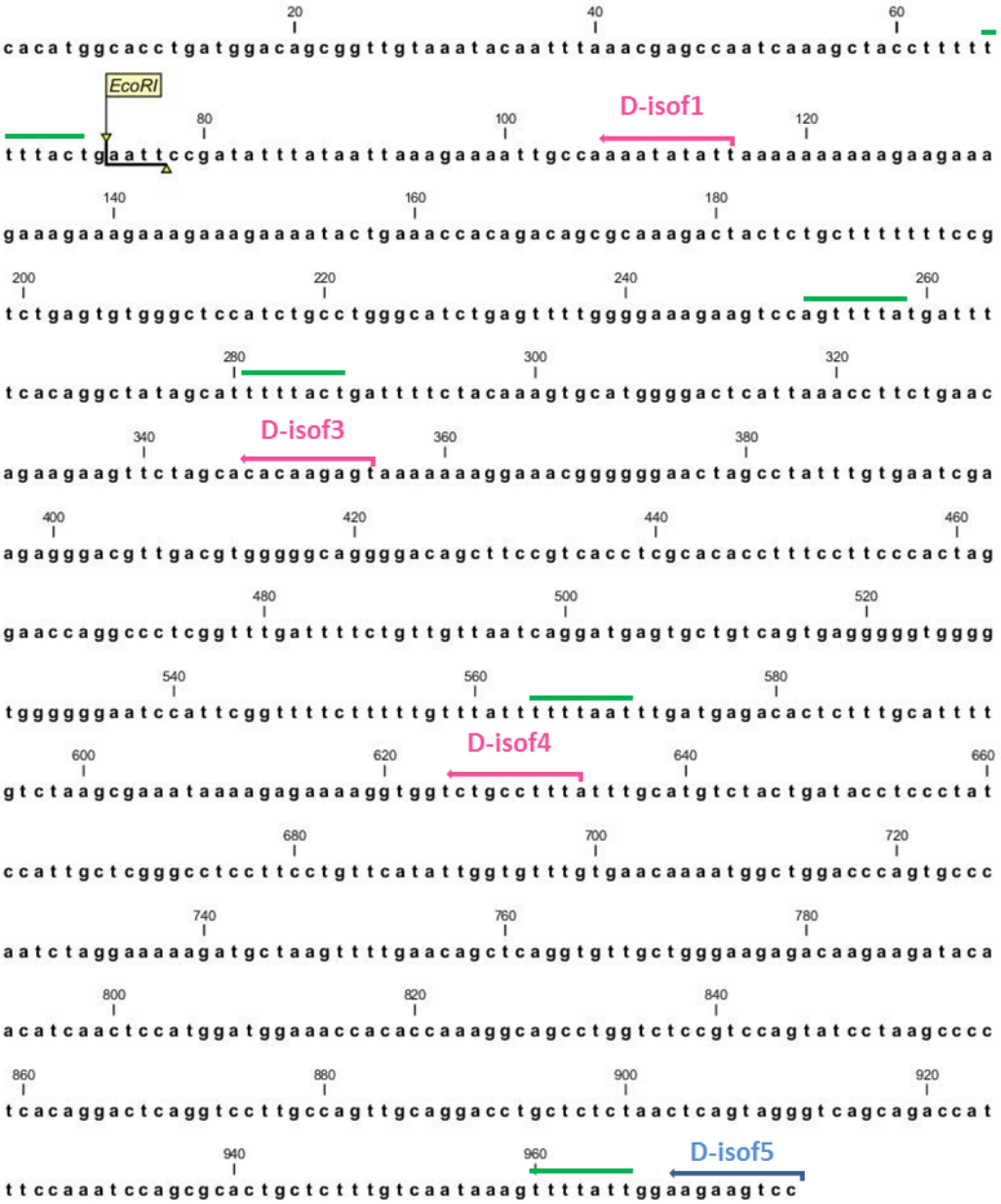

Figure 21: *DSCAM* isoforms 1, 3, 4 and 5 sequences.

DSCAM-isof1 (D-isof1) has 115 nucleotides in length and contains one CPE motif (TTTACT). *DSCAM*-isof3 (D-isof3) has 355 nucleotides in length and three CPE motifs (TTTACT, AGTTTTA, TTTTACT), *DSCAM*-isof4 (D-isof4) has 632 nucleotides and four CPE motifs (TTTACT, AGTTTTA, TTTTACT, TTTTAAT). *DSCAM*-isof5 (D-isof5) has 977 nucleotides and 5 CPE motifs (TTTACT, AGTTTTA, TTTTACT, TTTTAAT, TTTTATT). CPE motifs are marked with green lines. These isoforms are encoded in the same exon, and are originated by alternative polyadenylation. This graph was obtained using the free version of CLC Sequence Viewer program.

3.3 Preliminary visualization of DSCAM local translation using Kaede reporters

Hippocampal neurons were firstly transfected with the original pKaede MC1 plasmid to test protein expression and visualization in an epifluorescence microscope equipped for standard green and red fluorescence visualization. However, the excitation light to elicit green and red fluorescence in Kaede protein is very narrow, 508/518 and 572/580 respectively. For this reason we decided to use confocal microscopy because in this case, the specific Kaede parameters can be finely chosen. Two days after transfection using the original Kaede vector and the modified Kaede-3'UTR plasmid, neurons were observed. Kaede protein was visualized in the entire neuron (cell body, dendrites and axons; not shown). The modified Kaede-3'UTR plasmid permitted the expression of Kaede protein in a similar granular pattern as pKaede MC1 (Fig. 22 A). To assess the morphology of these granules, zoom amplification was made. Round distinct forms could be distinguished (Fig. 22 B and C). These images were used as controls to compare the expression of Kaede-based 3'UTR *DSCAM*-isoforms. For this purpose, the image in panel A was designed as the reporter control (RC) when the expression occurs in the entire neuron. The image in panel C was defined as the reporter control zoom (RCZ) and was used for comparison with Kaede-*DSCAM*-isoforms when the expression was localized in neurites (i. e., dendrites or axons).

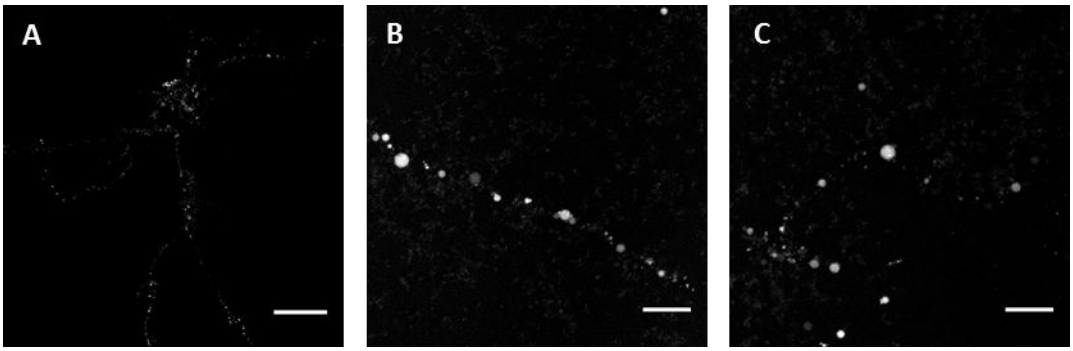

Figure 22: Visualization of Kaede reporters.

A) Kaede-3'UTR plasmid expression in a transfected neuron. Scale bar, 100 µm. B) and C) Zoom of different neurites of panel A. Scale bar, 10 µm.

To confirm that the fluorescence observed in experiments summarized in figure 22 was originated by the expression of Kaede, the photoconversion capacity of the protein was assessed. As shown in figure 23 decreasing of green fluorescence and increasing of red fluorescence was observed when neurons were subjected to succesive pulses of UV light.

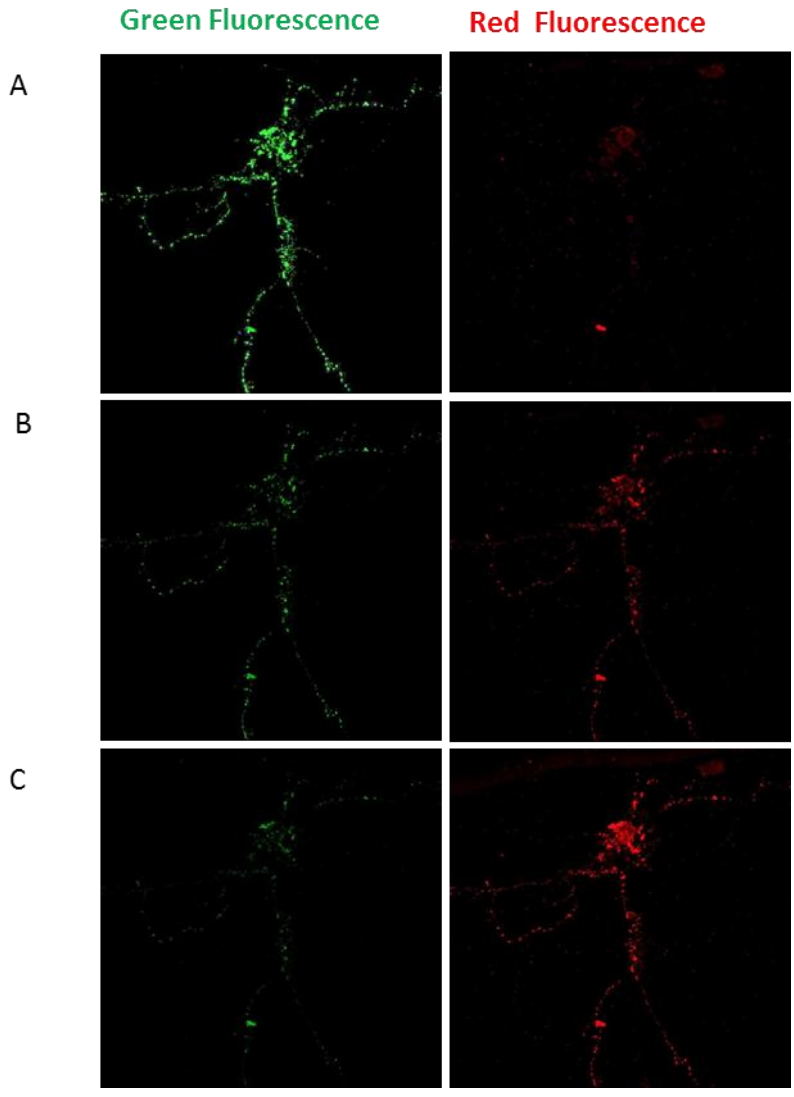

Figure 23: Visualization of Kaede photoconversion.

A) Initial image showing green and red fluorescence when pKaede-3'UTR plasmid was used for neuron transfection. B) Neurons after a 10 sec UV pulse. C) Neurons after a 20 sec UV pulse. (Total UV pulse= 30 sec).

To assess the impact of the different 3'UTR *DSCAM* isoforms on Kaede expression, we decided to transfect DIV7 hippocampal neurons with the corresponding plasmid. Phenotypes were analyzed 2 days later.

Kaede-*DSCAM*-isof1 expression apparently occurred in dendrites (and maybe axons) but the expression in neuron cell body was not detected (Fig. 24).

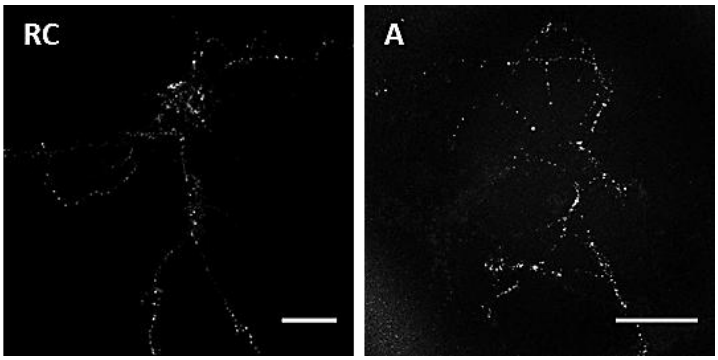

Figure 24: Kaede-*DSCAM*-isof1 expression.

RC) Reporter Control where neuron cell body and dendrites were visualized. Scale bar,100 µm. A) Expression of Kaede-*DSCAM*-isof1 in dendrites (and maybe axon). Note that expression was not detected in neuron cell body. Scale bar, 50 µm.

Kaede-*DSCAM*-isof3 expression was observed in dendrites and neuron cell body (Fig. 25). After a 20 sec UV pulse protein photoconversion was confirmed (Fig. 25, B1 and B2).

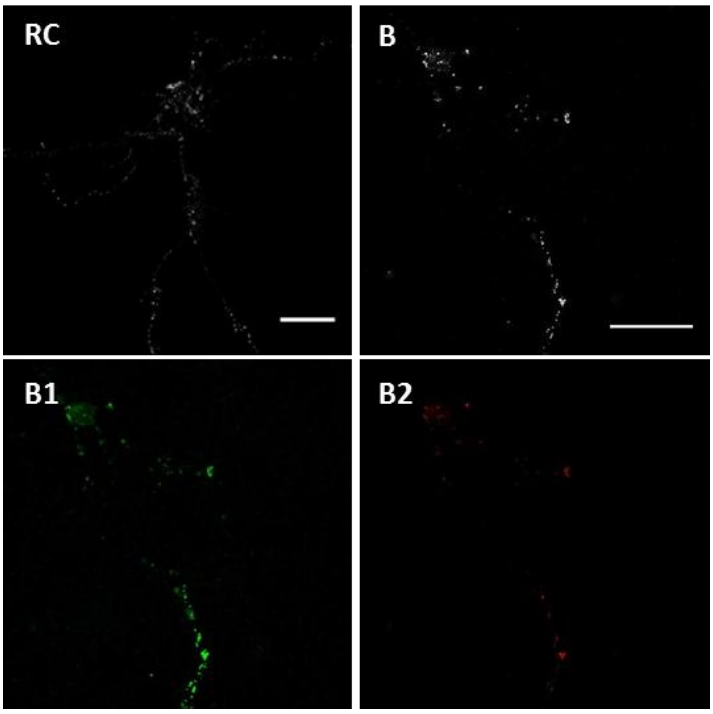

Figure 25: Kaede-*DSCAM*-isof3 expression.
RC) Reporter Control (same as fig. 22 A) where neuron cell body and dendrites were visualized. B) Expression of Kaede-*DSCAM*-isof3 in dendrites and in cell body. Scale bar, 50 µm. B1) Green fluorescence detection after a 20 sec UV pulse. B2) Red fluorescence visualization after a 20 sec UV pulse.

When Kaede-*DSCAM*-isof4 expression was analysed an aberrant morphology was visualized in all the transfected neurons (Fig. 26 and Fig. 27). In this case, a high Kaede expression that mainly occurred in neuron cell body was evident when compared with the expression of Kaede-*DSCAM*- isoforms 1, 3 and 5.

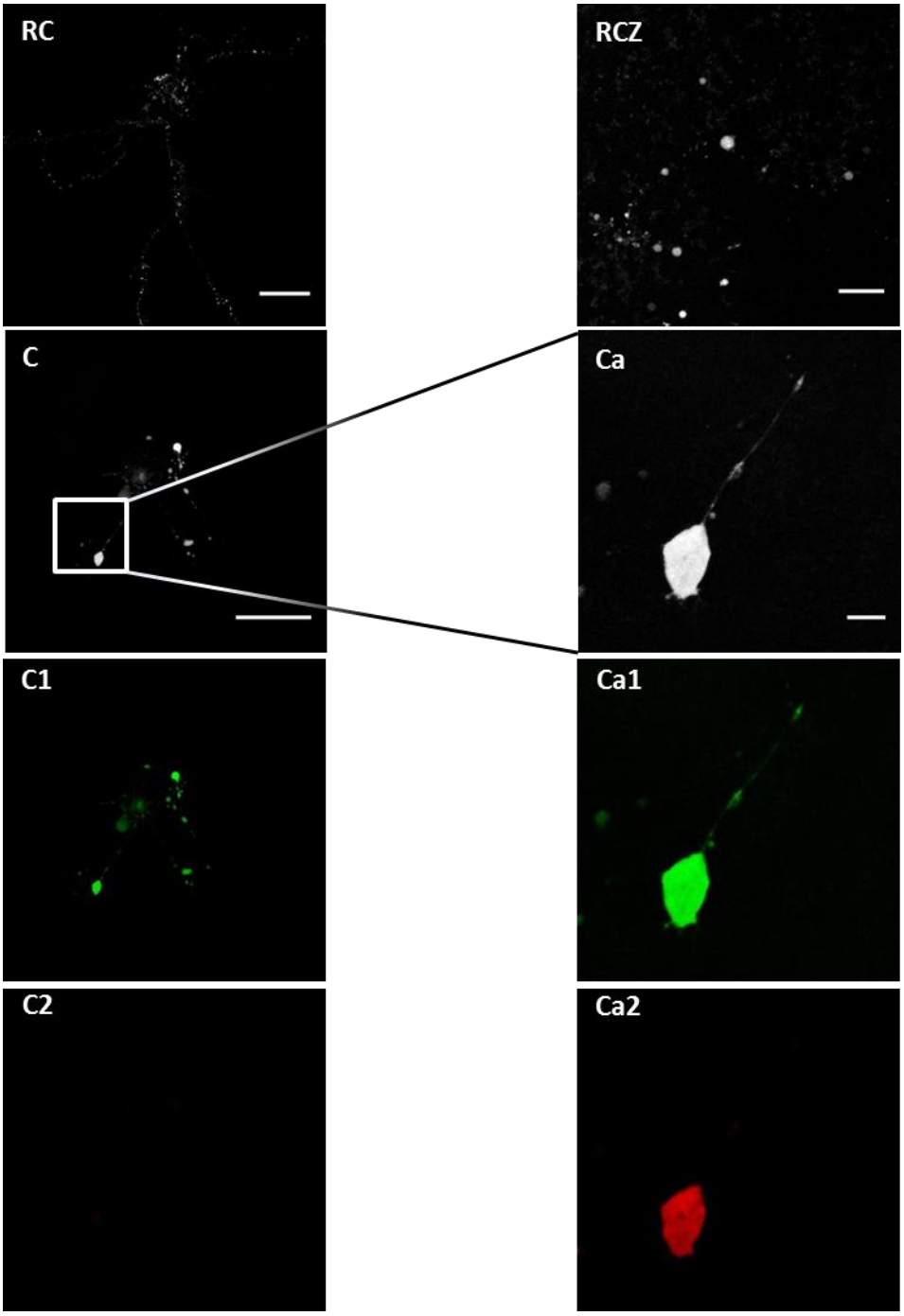

Figure 26: Kaede-*DSCAM*-isof4 expression.

RC) Reporter Control (same as Fig. 22 A) where neuron cell body and dendrites were visualized. Scale bar 100 µm. RCZ) Reporter Control Zoom (same as Fig. 22 C). Scale bar, 10 µm. C) Expression of Kaede-*DSCAM*-isof4. No evident cell body seems to be labeled in this image, although neurite labeling can be appreciated. Scale bar, 50 µm. C1) Green fluorescence before UV pulse. C2) Red fluorescence was not detected before UV pulse. Ca) Magnification of a Kaede-positive granule from panel C. Scale bar 10 µm. Ca1) Green fluorescence detection after a 20 sec UV pulse. Ca2) Red fluorescence detection after a 20 sec UV pulse.

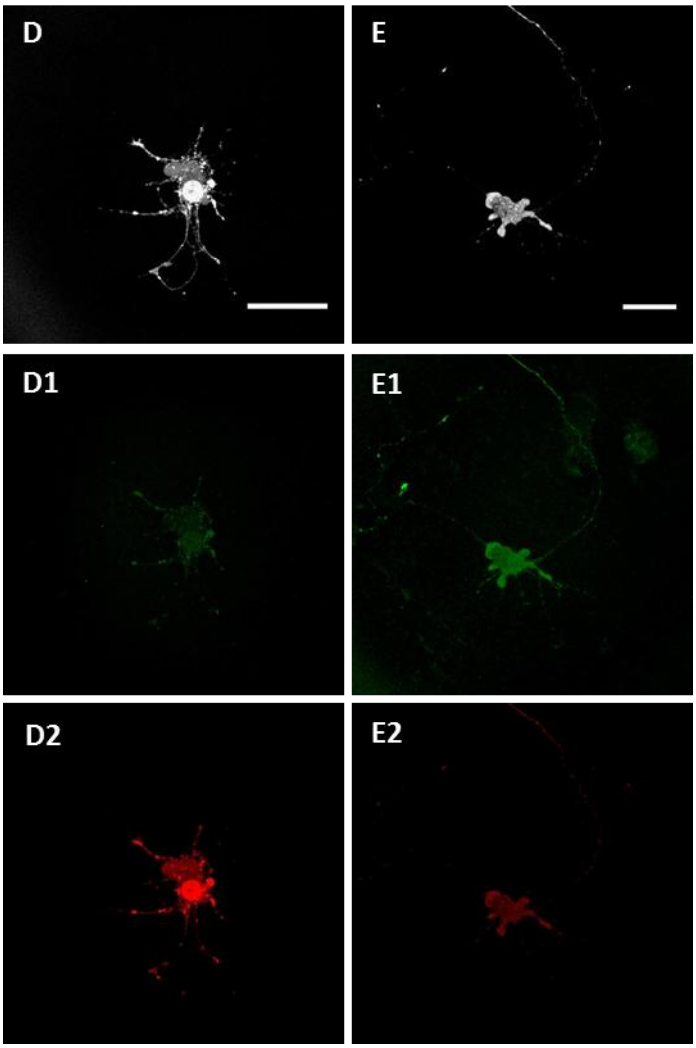

Figure 27: Kaede-*DSCAM*-isof4 expression (II).

Aberrant neuron morphology produced by transfection of pKaede-*DSCAM*-isof4. D) Cell body can be distinguished in this image. Expression of Kaede-*DSCAM*-isof4 is not strong in dendrites or axons. Scale bar, 50 µm. E) In this transfected neuron, cell body is strongly marked, and neuritis are also detected, although with less intensity. Scale bar, 100 µm. D1, E1) Detection of green fluorescence after a 20 sec UV pulse. D2, E2) Red fluorescence detection after a 20 sec UV pulse.

While the expression of Kaede-*DSCAM*-isof4 appears to be higher in the neuronal cell body and weakly detectable in dendrites and axons, Kaede-*DSCAM*-isof5 is apparently expressed in neurites. Thus, transfected neurons with pKaede-*DSCAM*-isof5 did not show expression in cell bodies, but presented a distinct morphological feature consisting in granules that delineated what seemed to be axons (Fig. 28).

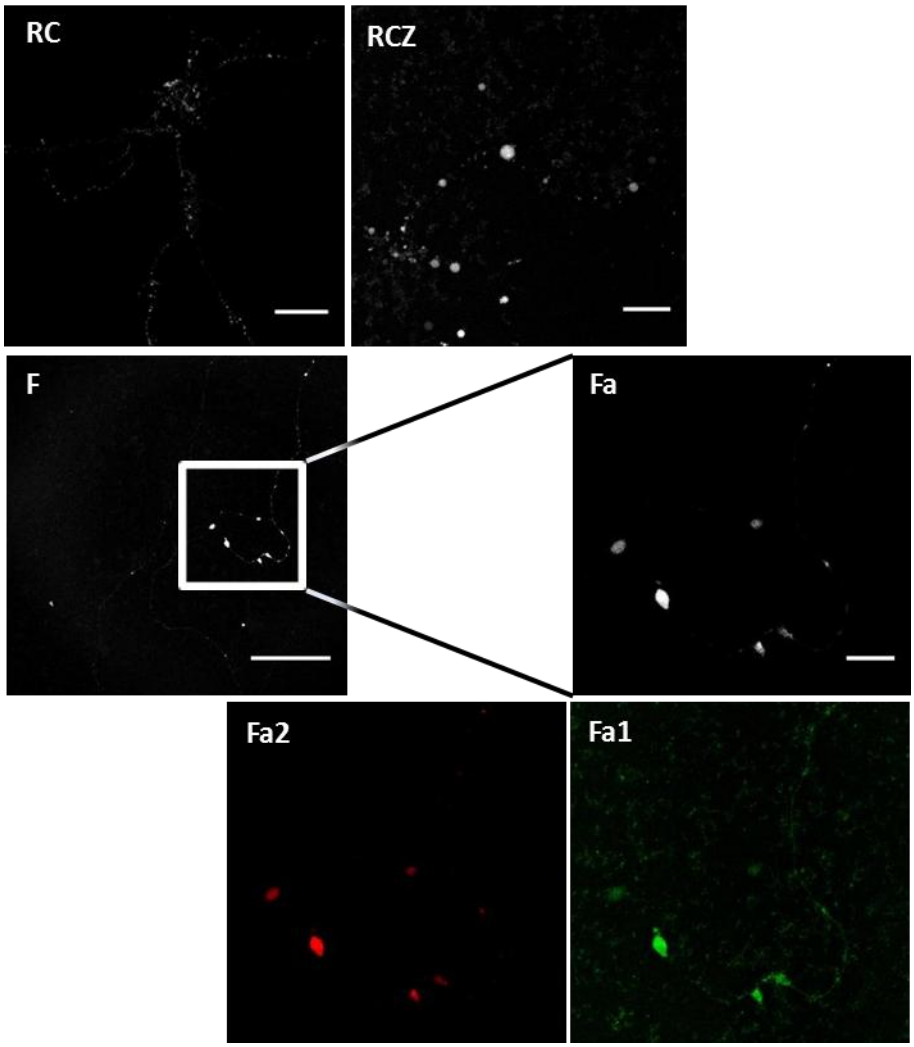

Figure 28: Kaede-*DSCAM*-isof5 expression.

RC) Reporter Control where neuron body cell and dendrites are visualized (same as Fig. 22 A). Scale bar, 100 µm. RCZ) Reporter Control Zoom (same as Fig. 22 C). Scale bar, 10 µm. F) Expression of pKaede-*DSCAM*-isof5 showing no cell body labeling; however, neurite labeling (probably an axon) is evident. Scale bar, 50 µm. Fa) Magnification from panel F. Fa1) Green fluorescence detection after a 20 sec UV pulse. Fa2) Red fluorescence detection after a 20 sec UV pulse

4. Discussion

In neurons certain mRNA transcripts are transported to dendrites for localized translation (Bramham and Wells, 2007). In the last years, one of the greatest challenges in local translation studies are the identification of mRNA localization and protein synthesis within discrete cell compartments (Martin and Ephrussi, 2009). We have described the visualization of DSCAM synthesis in postnatal hippocampal neurons, using the photoconvertible Kaede reporter protein.

The first visualization method that provided the initial evidence that dendrites are capable of autonomous translational control occurred by using transmission electron microscopy (TEM). Owing to its unique ability to resolve the fine intracellular structure of neurons, it has remained an important tool for understanding local protein synthesis in dendrites and its relationship to synaptic plasticity and memory (Ostroff et al., 2002). In a recent study using this technique, it has been demonstrated that fear conditioning increases both the number of dendritic polyribosomes and their association with the spine apparatus in lateral amygdala neurons. The observed increase in polyribosomes likely reflects an overall increase in dendritic translation after fear learning, although other interpretations cannot be fully ruled out (Ostroff et al., 2010). The major limitation of TEM is that changes in dendritic translation relative to baseline cannot be studied in the same sample. This deficiency prompted the development of methods to dynamically visualize local synthesis of proteins in neuronal processes. The first tools developed used a myristoylated green fluorescent protein (GFP) (Aakalu et al., 2001). This myristoylation signal provides an excellent advantage by allowing the reporter to attach the membrane, avoiding the protein diffusion through the whole cell. However, photobleaching is necessary for eliminating the signal from pre-existing GFP protein, as this technique is based in fluorescence after photobleaching (FRAP), and this may be toxic for the cells. The recovery of GFP fluorescence in dendrites following photobleaching is due to both diffusion from the adjacent (nonbleached) compartment as well as the new synthesis of the reporter in the bleached domain (Aakalu et al., 2001). This can lead to the visualization of increased fluorescence that does not reflect the real protein expression. Furthermore, there are FRAP experiment that describe that the rate of degradation of the reporter can exceeded the rate of diffusion of the reporter (Aakalu et al., 2001). This can lead to decreased fluorescence capture. Attending to this, the use of GFP in local translation experiments do not provide a mean to obtain trustable and clear results about new local protein expression.

In the present work, the Kaede-MC1 plasmid that encodes the photoconvertible fluorescent protein Kaede was used. It provides a mean of monitoring new local translation because all preexisting protein can be photoconverted from green to red, and then new translation can be monitored as the appearance of new green signal (Ando et al., 2002). Despite this ability, only the expression of Kaede and Kaede-*DSCAM*-isoforms in hippocampal neuron cultures was assessed here.

The preliminary results shown in this work represent a first approach to identify in which compartments of a single neuron *DSCAM* isoforms are expressed. Studies performed on the same isoforms, reported that isoforms 1, 3, and 5 appeared to be more abundant in the neonatal hippocampus than in adult tissues, suggesting their role in developmental processes. In what concerns to isoform 4 in P0 and adult tissues, similar levels of expression were found, suggesting that this isoform may play a predominant role in neuronal physiology (Alves-Sampaio et al., 2010). Attending to the documented expression of these four *DSCAM* isoforms in neonatal hippocampus, all of them were expected to be expressed in this experimental approach. The next table summarizes the localized compartments where the expression of the different constructions in single neurons was observed. Due to the difficulty for distinguish some neuronal cell compartments, all the fluorescence observed in continuous or discontinuous points (granules), were assumed to be dendrites and/or axons.

Table 4: Localization overview of Kaede and Kaede-*DSCAM*-isoforms expression.

Reporter/ DNA constructions	Neuronal Compartment	
	Cell body	Dendrites/ Axons
Kaede	√	√
Kaede-3'UTR	√	√
Kaede-*DSCAM*-isof1	–	√
Kaede-*DSCAM*-isof3	√	√
Kaede-*DSCAM*-isof4	√	–
Kaede-*DSCAM*-isof5	–	√

Kaede-*DSCAM*-isof1 expression apparently occurred in dendrites or axon but the expression in neuron cell body was not identified. The same happened with Kaede-*DSCAM*-isof5. However, the morphology of the Kaede granules seemed to be different in both cases. Thus, whereas granules were large and oval-shaped in the case of Kaede-*DSCAM*-isof5, they were round and small in the case of Kaede-*DSCAM*-isof1. This suggests that these isoforms may be transported from the soma in RNA granules and regulated translation may occur by different mechanisms during the transport. For instance, in the case of mammalian Staufen proteins, there is biochemical evidence that some RNA granules contain ribosomes, whereas others do not. When fractionated by size, the largest Staufen pools contained ribosomal and endoplasmic reticulum (ER) markers, whereas the smaller RNA granules were free of ribosomes and ER but cofractionated with conventional kinesin (Mallardo et al., 2003). Furthermore, it is assumed that during transport mRNAs might be translationally repressed within granules but studies also report that mRNAs can be released from the granules, and/or be derepressed in response to neuronal activity, allowing for local translation (Krichevsky and Kosik, 2001, Huttelmaier et al., 2005).

Kaede-DSCAM-isof3 expression was observed in dendrites and neuron cell body. This suggests that the translation of this isoform may be regulated by several mechanisms. First, after Kaede-DSCAM-isof3 translation in the soma, the new synthetized protein may be transported to the dendrites. Second, mRNA may be transported from the soma to the dendrites and being translated in this way, leaving a footprint in form of synthetized protein. Finally, due to the similarity of expression between Kaede and Kaede-DSCAM-isof3, the possibility of having problems with the plasmid that may lead to DSCAM-isof3 incorrect translation, have to be taken in count.

In the case of kaede-*DSCAM*-isof4 an aberrant morphology was visualized. In this case, high Kaede expression occurred in neuron cell body when compared with the expression of Kaede-*DSCAM*-isoforms 1, 3 or 5. The overexpression appears to confer a kind of apoptotic neuronal feature. DSCAM-isof4 contains four CPE motifs (TTTACT, AGTTTTA, TTTTACT, TTTTAAT) that are expected to be recognized by CPEB proteins. Interestingly, recent works have shown that CPEB also coordinates the translation regulation of p53 mRNA (Richter et al., 2011) a tumor suppressor and transcription factor that is a key modulator of cellular stress responses (Culmsee and Mattson, 2005). Besides polyadenylation sites, CPEB 3' UTR contains two miR-122 binding sites, which when deleted, elevate mRNA translation. Although miR-122 is thought to be liver specific, it is present in primary fibroblasts and destabilized by Gld2 depletion. Gld4, a second non-

canonical poly(A) polymerase, was found to regulate p53 mRNA polyadenylation/translation in a CPEB-dependent manner. Thus, translational regulation of p53 mRNA and cellular senescence is coordinated by Gld2/miR-122/CPEB/Gld4 (Richter et al., 2011). Activation of p53 can trigger apoptosis in many cell types including neurons (Culmsee and Mattson, 2005). This suggest that CPEB controls senescence and bioenergetics in human cells at least in part by modulating p53 mRNA polyadenylation-induced translation (Richter and Burns, 2008) and, attending to the results, expression of DSCAM-isof4 may trigger this activation. However, improvements of the experiment should be made to obtain more reliable and consistent results.

Some of these improvements imply Kaede plasmid modification. The Kaede plasmid used to insert DSCAM isoforms 1, 3, 4 and 5 do not have stop codons. This could have led to altered protein conformation and the absence of Kaede fluorescence after synthesis. However, as demonstrated in the point 3.3 of this work, photoconversion occurs after a 20sec UV pulse, confirming that the His-Tyr-Gly chromophore did not suffered modifications. Even so, in the plasmid Kaede-3'UTR, a myristoylation signal that inhibits the free diffusion of the reporter (Aakalu et al., 2001) should be added. Furthermore, a polylinker at the 5' UTR of Kaede protein could also be added allowing the possibility of cloning the 5'UTR of *DSCAM* isoforms that may also contain DTEs and other regulatory sequences. Due to the polyadenylation signals of *DSCAM* are in tandem, *DSCAM*-isoform 5 plasmid can also produce the 3'UTR of *DSCAM* Isoforms 1, 3 and 4. This could be overtaken by constructing synthetic mRNAs and instead of transfection, another method like microinjection of mRNA-based reporters could be used.

mRNAs that are important for LTP might be a different or overlapping population from those that are required for LTD, but both are presumably present in the same region of the dendrite (Bramham and Wells, 2007). The remaining question is how selective mRNAs are activated while others remain dormant. The answer might reside in the presence of RNA-binding proteins (ZBP1, CPEB and FMRP) that bind to specific cis-elements (DTEs) and are capable of regulating mRNA translation. One example of this type of regulation is the regulation of β-actin mRNA by ZBP1. Studies performed in chicken, reported that ZBP1 modulates the translation of b-actin mRNA. ZBP1 associates with the b-actin transcript in the nucleus and prevents premature translation in the cytoplasm by blocking translation initiation. Translation only occurs when the ZBP1–RNA complex reaches its destination at the periphery of the cell. At the endpoint of mRNA

transport, the protein kinase Src promotes translation by phosphorylating a key tyrosine residue in ZBP1 that is required for binding to RNA (Huttelmaier et al., 2005). The dynamic movements of ZPB1 in response to KCl-induced depolarization at high spatial and temporal resolution (Tiruchinapalli et al., 2003) also implicate RNA binding proteins as regulators of mRNA transport to activated synapses in response to synaptic activity. So, for obtaining more clues about the regulation of DSCAM by RNA-binding proteins, neuron stimulation should be performed and live visualization of DSCAM expression could be monitored.

The application of the methodology described in this work with the suggested improvements in Ts1Cje or Ts65Dn trissomic mice, may lead to more precise results about the role of DSCAM in DS.

5. Conclusion and perspectives

In conclusion, the four different isoforms have distinct expression locations in neurons. Kaede-*DSCAM*-isof1 is expressed in neurites (dendrites and axons) but not in cell body whereas Kaede-*DSCAM*-isof3 appears to be expressed in both compartments. Kaede-*DSCAM*-isof4 expression appears to confer a rare morphological feature to neuron cell body were it is highly expressed. Expression of Kaede-*DSCAM*-isof5 is visualized in oval granules continuously connected in what appears to be an axon. The results presented in this work with hippocampal neurons shows that DSCAM isoform 1 may be repressed at the soma, DSCAM isoform 3 appear not to be specifically regulated and isoforms 4 and 5 appear to be repressed and activated (strong activated in case of isoform 4 and weakly activated in case of isoform 5). So, the regulation of isoforms 4 and 5 fitted the CPE code unlike the predicted behaviour for DSCAM isoforms 1 and 3.

Although synaptic stimulation was not performed in this work, the use of Kaede as a local translation reporter, represents a reliable strategy for visualize *DSCAM* local expression in hippocampal neuron cultures. However, some improvements that imply Kaede plasmid modification should be performed., A myristoylation signal that inhibits the free diffusion of the reporter (Aakalu et al., 2001) should be added to the plasmid Kaede-3'UTR obtained in this work. Furthermore, a polylinker at the 5' UTR of Kaede protein could also be added allowing the possibility of cloning the 5'UTR of *DSCAM* isoforms that may also contain DTEs and other regulatory sequences. So, for obtaining even more clues about the regulation of DSCAM by RNA-binding proteins, neuron stimulation should be performed and live visualization of DSCAM isoforms expression could be monitored.

The application of the methodology described in this work with the suggested improvements in Ts1Cje or Ts65Dn trissomic mice, may also lead to more precise and valuable results about the role of DSCAM in DS.

6. References

Aakalu G, Smith WB, Nguyen N, Jiang C, Schuman EM (2001) Dynamic Visualization of Local Protein Synthesis in Hippocampal Neurons. Neuron 30:489-502.

Abbeduto L, Warren SF, Conners FA (2007) Language development in down syndrome: From the prelinguistic period to the acquisition of literacy. Ment Retard Dev D R 13:247-261.

Agarwala KL, Ganesh S, Amano K, Suzuki T, Yamakawa K (2001) DSCAM, a highly conserved gene in mammals, expressed in differentiating mouse brain. Biochem Bioph Res Co 281:697-705.

Agarwala KL, Nakamura S, Tsutsumi Y, Yamakawa K (2000) Down syndrome cell adhesion molecule DSCAM mediates homophilic intercellular adhesion. Molecular Brain Research 79:118-126.

Alves-Sampaio A, Troca-Marin JA, Montesinos ML (2010) NMDA-Mediated Regulation of DSCAM Dendritic Local Translation Is Lost in a Mouse Model of Down's Syndrome. J Neurosci 30:13537-13548.

Anderson P, Kedersha N (2006) RNA granules. J Cell Biol 172:803-808.

Ando R, Hama H, Yamamoto-Hino M, Mizuno H, Miyawaki A (2002) An optical marker based on the UV-induced green-to-red photoconversion of a fluorescent protein. Proceedings of the National Academy of Sciences of the United States of America 99:12651-12656.

Barlow GM, Lyons GE, Korenberg JR (2001) Down syndrome cell adhesion molecule (DSCAM): a role in spinal cord differentiation and cortical plasticity? American Journal of Human Genetics 69:341-341.

Bassell GJ, Warren ST (2008) Fragile X Syndrome: Loss of Local mRNA Regulation Alters Synaptic Development and Function. Neuron 60:201-214.

Benavides-Piccione R, Ballesteros-Yáñez I, Martínez de Lagrán M, Elston G, Estivill X, Fillat C, DeFelipe J, Dierssen M (2004) On dendrites in Down syndrome and DS murine models: a spiny way to learn. Progress in Neurobiology 74:111-126.

Blichenberg A, Schwanke B, Rehbein M, Garner CC, Richter D, Kindler S (1999) Identification of a cis-acting dendritic targeting element in MAP2 mRNAs. J Neurosci 19:8818-8829.

Bourne JN, Harris KM (2008) Balancing structure and function at hippocampal dendritic spines. Annu Rev Neurosci 31:47-67.

Bramham CR, Wells DG (2007) Dendritic mRNA: transport, translation and function. Nat Rev Neurosci 8:776-789.

Brown V, Jin P, Ceman S, Darnell JC, O'Donnell WT, Tenenbaum SA, Jin XK, Feng Y, Wilkinson KD, Keene JD, Darnell RB, Warren ST (2001) Microarray identification of FMRP-associated brain mRNAs and altered mRNA translational profiles in fragile X syndrome. Cell 107:477-487.

Browne GJ, Proud CG (2002) Regulation of peptide-chain elongation in mammalian cells. Eur J Biochem 269:5360-5368.

Burgess RW, Fuerst PG, Bruce F, Tian M, Wei W, Elstrott J, Feller MB, Erskine L, Singer JH (2009) DSCAM and DSCAML1 Function in Self-Avoidance in Multiple Cell Types in the Developing Mouse Retina. Neuron 64:484-497.

Chalberg TW, Phillips JE, Calos MP (2001) Transfection of DNA into Mammalian Cells in Culture: John Wiley & Sons, Ltd.

Culmsee C, Mattson MP (2005) p53 in neuronal apoptosis. Biochem Bioph Res Co 331:761-777.

Dictenberg JB, Swanger SA, Antar LN, Singer RH, Bassell GJ (2008) A direct role for FMRP in activity-dependent dendritic mRNA transport links filopodial-spine morphogenesis to fragile X syndrome. Dev Cell 14:926-939.

Epstein CJ (2002) From Down syndrome to the "human" in "human genetics". American Journal of Human Genetics 70:300-313.

Farhood H, Gao X, Son K, Yang YY, Lazo JS, Huang L, Barsoum J, Bottega R, Epand RM (1994) Cationic Liposomes for Direct Gene-Transfer in Therapy of Cancer and Other Diseases. Ann Ny Acad Sci 716:23-35.

Fuerst PG, Koizumi A, Masland RH, Burgess RW (2008) Self-avoidance mediated by DSCAM in the developing mammalian retina. Int J Dev Neurosci 26:832-832.

Garber K, Smith KT, Reines D, Warren ST (2006) Transcription, translation and fragile X syndrome. Curr Opin Genet Dev 16:270-275.

Gardiner KJ (2010) Molecular basis of pharmacotherapies for cognition in Down syndrome. Trends Pharmacol Sci 31:66-73.

Gibson JR, Bartley AF, Hays SA, Huber KM (2008) Imbalance of Neocortical Excitation and Inhibition and Altered UP States Reflect Network Hyperexcitability in the Mouse Model of Fragile X Syndrome. J Neurophysiol 100:2615-2626.

Grafstein B, Forman DS (1980) Intracellular-Transport in Neurons. Physiol Rev 60:1167-1283.

Graham FL, Vandereb AJ (1973) Transformation of Rat Cells by DNA of Human Adenovirus-5. Virology 54:536-539.

Hassold T, Hall H, Hunt P (2007) The origin of human aneuploidy: where we have been, where we are going. Human Molecular Genetics 16:R203-R208.

Hattori M, Fujiyama A, Taylor TD, Watanabe H, Yada T, Park HS, Toyoda A, Ishii K, Totoki Y, Choi DK, Soeda E, Ohki M, Takagi T, Sakaki Y, Taudien S, Blechschmidt K, Polley A, Menzel U, Delabar J, Kumpf K, Lehmann R, Patterson D, Reichwald K, Rump A, Schillhabel M, Schudy A, Zimmermann W, Rosenthal A, Kudoh J, Shibuya K, Kawasaki K, Asakawa S, Shintani A, Sasaki T, Nagamine K, Mitsuyama S, Antonarakis SE, Minoshima S, Shimizu N, Nordsiek G, Hornischer K, Brandt P, Scharfe M, Schon O, Desario A, Reichelt J, Kauer G, Blocker H, Ramser J, Beck A, Klages S, Hennig S, Riesselmann L, Dagand E, Haaf T, Wehrmeyer S, Borzym K, Gardiner K, Nizetic D, Francis F, Lehrach H, Reinhardt R, Yaspo ML, Groner Y, consortium Cms (2000) The DNA sequence of human chromosome 21. Nature 405:311-319.

Holbro N, Grunditz A, Oertner TG (2009) Differential distribution of endoplasmic reticulum controls metabotropic signaling and plasticity at hippocampal synapses. Proceedings of the National Academy of Sciences of the United States of America 106:15055-15060.

Hou LF, Antion MD, Hu DY, Spencer CM, Paylor R, Klann E (2006) Dynamic translational and proteasomal regulation of fragile X mental retardation protein controls mGluR-dependent long-term depression. Neuron 51:441-454.

Huang YS, Carson JH, Barbarese E, Richter JD (2003) Facilitation of dendritic mRNA transport by CPEB. Gene Dev 17:638-653.

Huang YS, Jung MY, Sarkissian M, Richter JD (2002) N-methyl-D-aspartate receptor signaling results in Aurora kinase-catalyzed CPEB phosphorylation and alpha CaMKII mRNA polyadenylation at synapses. Embo J 21:2139-2148.

Huang YS, Kan MC, Lin CL, Richter JD (2006) CPEB3 and CPEB4 in neurons: analysis of RNA-binding specificity and translational control of AMPA receptor GluR2 mRNA. Embo J 25:4865-4876.

Huttelmaier S, Zenklusen D, Lederer M, Dictenberg J, Lorenz M, Meng XH, Bassell GJ, Condeelis J, Singer RH (2005) Spatial regulation of beta-actin translation by Src-dependent phosphorylation of ZBP1. Nature 438:512-515.

Irwin SA, Patel B, Idupulapati M, Harris JB, Crisostomo RA, Larsen BP, Kooy F, Willems PJ, Cras P, Kozlowski PB, Swain RA, Weiler IJ, Greenough WT (2001) Abnormal dendritic spine characteristics in the temporal and visual cortices of patients with fragile-X syndrome: A quantitative examination. Am J Med Genet 98:161-167.

Jin P, Warren ST (2000) Understanding the molecular basis of fragile X syndrome. Human Molecular Genetics 9:901-908.

Ju W, Morishita W, Tsui J, Gaietta G, Deerinck TJ, Adams SR, Garner CC, Tsien RY, Ellisman MH, Malenka RC (2004) Activity-dependent regulation of dendritic synthesis and trafficking of AMPA receptors. Nat Neurosci 7:244-253.

Kandel ER (2001) The molecular biology of memory storage: A dialog between genes and synapses. Bioscience Rep 21:565-611.

Kiebler MA, Bassell GJ (2006) Neuronal RNA granules: Movers and makers. Neuron 51:685-690.

Kim HK, Kim YB, Kim EG, Schuman E (2005) Measurement of dendritic mRNA transport using ribosomal markers. Biochem Bioph Res Co 328:895-900.

Kirov SA, Harris KM (1999) Dendrites are more spiny on mature hippocampal neurons when synapses are inactivated. Nat Neurosci 2:878-883.

Klann E, Dever TE (2004) Biochemical mechanisms for translational regulation in synaptic plasticity. Nat Rev Neurosci 5:931-942.

Kobayashi H, Yamamoto S, Maruo T, Murakami F (2005) Identification of a cis-acting element required for dendritic targeting of activity-regulated cytoskeleton-associated protein mRNA. Eur J Neurosci 22:2977-2984.

Kotaleski JH, Blackwell KT (2010) Modelling the molecular mechanisms of synaptic plasticity using systems biology approaches. Nat Rev Neurosci 11:239-251.

Krichevsky AM, Kosik KS (2001) Neuronal RNA granules: A link between RNA localization and stimulation-dependent translation. Neuron 32:683-696.

Malenka RC, Bear MF (2004) LTP and LTD: An embarrassment of riches. Neuron 44:5-21.

Malenka RC, Nicoll RA (1997) Learning and memory - Never fear, LTP is hear. Nature 390:552-553.

Mallardo M, Deitinghoff A, Muller J, Goetze B, Macchi P, Peters C, Kiebler MA (2003) Isolation and characterization of Staufen-containing ribonucleoprotein particles from rat brain. Proceedings of the National Academy of Sciences of the United States of America 100:2100-2105.

Martin KC, Ephrussi A (2009) mRNA Localization: Gene Expression in the Spatial Dimension. Cell 136:719-730.

Mendez R, Murthy KGK, Ryan K, Manley JL, Richter JD (2000) Phosphorylation of CPEB by Eg2 mediates the recruitment of CPSF into an active cytoplasmic polyadenylation complex. Mol Cell 6:1253-1259.

Mendez R, Richter JD (2001) Translational control by CPEB: A means to the end. Nat Rev Mol Cell Bio 2:521-529.

Nadel L (2003) Down's syndrome: a genetic disorder in biobehavioral perspective. Genes Brain Behav 2:156-166.

Narayanan U, Nalavadi V, Nakamoto M, Pallas DC, Ceman S, Bassell GJ, Warren ST (2007) FMRP phosphorylation reveals an immediate-early signaling pathway triggered by group I mGluR and mediated by PP2A. J Neurosci 27:14349-14357.

Narayanan U, Nalavadi V, Nakamoto M, Thomas G, Ceman S, Bassell GJ, Warren ST (2008) S6K1 phosphorylates and regulates fragile X mental retardation protein (FMRP) with the neuronal protein synthesis-dependent mammalian target of rapamycin (mTOR) signaling cascade. Journal of Biological Chemistry 283:18478-18482.

Ostroff LE, Cain CK, Bedont J, Monfils MH, LeDoux JE (2010) Fear and safety learning differentially affect synapse size and dendritic translation in the lateral amygdala. Proceedings of the National Academy of Sciences of the United States of America 107:9418-9423.

Ostroff LE, Fiala JC, Allwardt B, Harris KM (2002) Polyribosomes redistribute from dendritic shafts into spines with enlarged synapses during LTP in developing rat hippocampal slices. Neuron 35:535-545.

Park S, Park JM, Kim S, Kim JA, Shepherd JD, Smith-Hicks CL, Chowdhury S, Kaufmann W, Kuhl D, Ryazanov AG, Huganir RL, Linden DJ, Worley PF (2008) Elongation factor 2 and fragile X mental retardation protein control the dynamic translation of Arc/Arg3.1 essential for mGluR-LTD. Neuron 59:70-83.

Perkel DJ, Petrozzino JJ, Nicoll RA, Connor JA (1993) The Role of Ca2+ Entry Via Synaptically Activated Nmda Receptors in the Induction of Long-Term Potentiation. Neuron 11:817-823.

Raab-Graham KF, Jan LY, Haddick PCG, Jan YN (2006) Activity- and mTOR-dependent suppression of Kv1.1 channel mRNA translation in dendrites. Science 314:144-148.

Rachidi M, Lopes C (2008) Mental retardation and associated neurological dysfunctions in Down syndrome: A consequence of dysregulation in critical chromosome 21 genes and associated molecular pathways. Eur J Paediatr Neuro 12:168-182.

Richter JD, Burns DM (2008) CPEB regulation of human cellular senescence, energy metabolism, and p53 mRNA translation. Gene Dev 22:3449-3460.

Richter JD, Burns DM, D'Ambrogio A, Nottrott S (2011) CPEB and two poly(A) polymerases control miR-122 stability and p53 mRNA translation. Nature 473:105-U125.

Richter JD, Kim JH (2006) Opposing polymerase-deadenylase activities regulate cytoplasmic polyadenylation. Mol Cell 24:173-183.

Richter JD, Sonenberg N (2005) Regulation of cap-dependent translation by eIF4E inhibitory proteins. Nature 433:477-480.

Rudelli RD, Wisniewski KE, Segan SM, Miezejeski CM, Sersen EA (1991) The Fra(X) Syndrome - Neurological, Electrophysiological, and Neuropathological Abnormalities. Am J Med Genet 38:476-480.

Saito Y, Oka A, Mizuguchi M, Motonaga K, Mori Y, Becker LE, Arima K, Miyauchi J, Takashima S (2000) The developmental and aging changes of Down's syndrome cell adhesion molecule expression in normal and Down's syndrome brains. Acta Neuropathologica 100:654-664.

Schmucker D, Chen B (2009) Dscam and DSCAM: complex genes in simple animals, complex animals yet simple genes. Gene Dev 23:147-156.

Siddiqui A, Lacroix T, Stasko MR, Scott-McKean JJ, Costa ACS, Gardiner KJ (2008) Molecular responses of the Ts65Dn and Ts1Cje mouse models of Down syndrome to MK-801. Genes Brain Behav 7:810-820.

Smith WB, Starck SR, Roberts RW, Schuman EM (2005) Dopaminergic stimulation of local protein synthesis enhances surface expression of GluR1 and synaptic transmission in hippocampal neurons. Neuron 45:765-779.

Steward O, Levy WB (1982) Preferential Localization of Polyribosomes under the Base of Dendritic Spines in Granule Cells of the Dentate Gyrus. J Neurosci 2:284-291.

Sutton MA, Wall NR, Aakalu GN, Schuman EM (2004) Regulation of dendritic protein synthesis by miniature synaptic events. Science 304:1979-1983.

Takashima S, Becker LE, Chan FW (1982) Retardation of Neuronal Maturation in Premature-Infants Compared with Term Infants of the Same Post-Conceptional Age. Pediatrics 69:33-39.

Theis M, Si K, Kandel ER (2003) Two previously undescribed members of the mouse CPEB family of genes and their inducible expression in the principal cell layers of the hippocampus. Proceedings of the National Academy of Sciences of the United States of America 100:9602-9607.

Tiruchinapalli DM, Oleynikov Y, Kelic S, Shenoy SM, Hartley A, Stanton PK, Singer RH, Bassell GJ (2003) Activity-dependent trafficking and dynamic localization of zipcode binding protein 1 and beta-actin mRNA in dendrites and spines of hippocampal neurons. J Neurosci 23:3251-3261.

Van Vactor D, Loya CM, Fulga TA (2010) Understanding neuronal connectivity through the post-transcriptional toolkit. Gene Dev 24:625-635.

Verkerk AJMH, Pieretti M, Sutcliffe JS, Fu YH, Kuhl DPA, Pizzuti A, Reiner O, Richards S, Victoria MF, Zhang FP, Eussen BE, Vanommen GJB, Blonden LAJ, Riggins GJ, Chastain JL, Kunst CB, Galjaard H, Caskey CT, Nelson DL, Oostra BA, Warren ST (1991) Identification of a Gene (Fmr-1) Containing a Cgg Repeat Coincident with a Breakpoint Cluster Region Exhibiting Length Variation in Fragile-X Syndrome. Cell 65:905-914.

Wang DO, Martin KC, Kim SM, Zhao YL, Hwang H, Miura SK, Sossin WS (2009) Synapse- and Stimulus-Specific Local Translation During Long-Term Neuronal Plasticity. Science 324:1536-1540.

Waung MW, Pfeiffer BE, Nosyreva ED, Ronesi JA, Huber KM (2008) Rapid translation of Arc/Arg3.1 selectively mediates mGluR-dependent LTD through persistent increases in AMPAR endocytosis rate. Neuron 59:84-97.

Weiler IJ, Irwin SA, Klintsova AY, Spencer CM, Brazelton AD, Miyashiro K, Comery TA, Patel B, Eberwine J, Greenough WT (1997) Fragile X mental retardation protein is translated near synapses in response to neurotransmitter activation. Proceedings of the National Academy of Sciences of the United States of America 94:5395-5400.

Wells DG, Dong X, Quinlan EM, Huang YS, Bear MF, Richter JD, Fallon JR (2001) A role for the cytoplasmic polyadenylation element in NMDA receptor-regulated mRNA translation in neurons. J Neurosci 21:9541-9548.

Wells DG, McEvoy M, Cao G, Llopis PM, Kundel M, Jones K, Hofler C, Shin C (2007) Cytoplasmic polyadenylation element binding protein 1-mediated mRNA translation in Purkinje neurons is required for cerebellar long-term depression and motor coordination. J Neurosci 27:6400-6411.

Westmark CJ, Malter JS (2007) FMRP mediates mGluR(5)-dependent translation of amyloid precursor protein. Plos Biol 5:629-639.

Wiseman FK, Alford KA, Tybulewicz VLJ, Fisher EMC (2009) Down syndrome-recent progress and future prospects. Human Molecular Genetics 18:R75-R83.

Wu L, Wells D, Tay J, Mendis D, Abbott MA, Barnitt A, Quinlan E, Heynen A, Fallon JR, Richter JD (1998) CPEB-mediated cytoplasmic polyadenylation and the regulation of experience-dependent translation of alpha-CaMKII mRNA at synapses. Neuron 21:1129-1139.

Yamakawa K, Huo YK, Haendel MA, Hubert R, Chen XN, Lyons GE, Korenberg JR (1998) DSCAM: a novel member of the immunoglobulin superfamily maps in a Down syndrome region and is involved in the development of the nervous system. Human Molecular Genetics 7:227-237.

Yamashima T, Popivanova B, Guo JZ, Mukaida N (2007) DSCAM in the hippocampal neurogenesis of ischemic monkeys. Neurosci Res 58:S57-S57.

Appendix

Alignment of DSCAM isoform 1 sequence with the constructed Kaede-DSCAM-isoform 1.

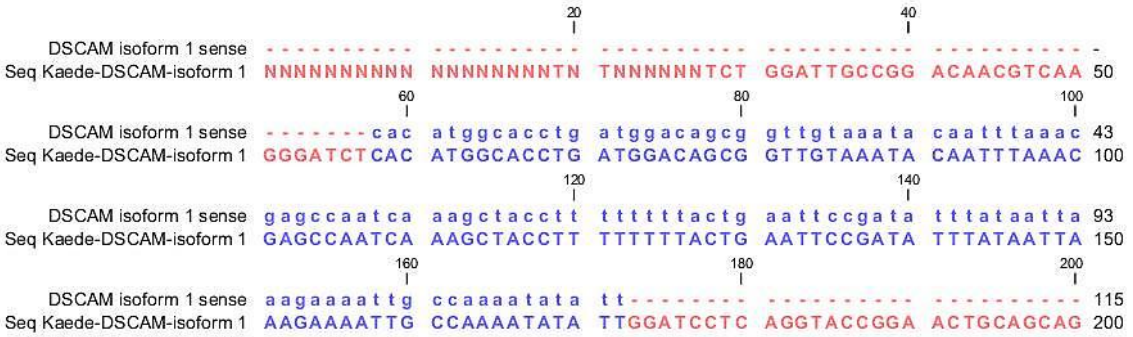

Alignment of DSCAM isoform 3 sequence with the constructed Kaede-DSCAM-isoform 3.

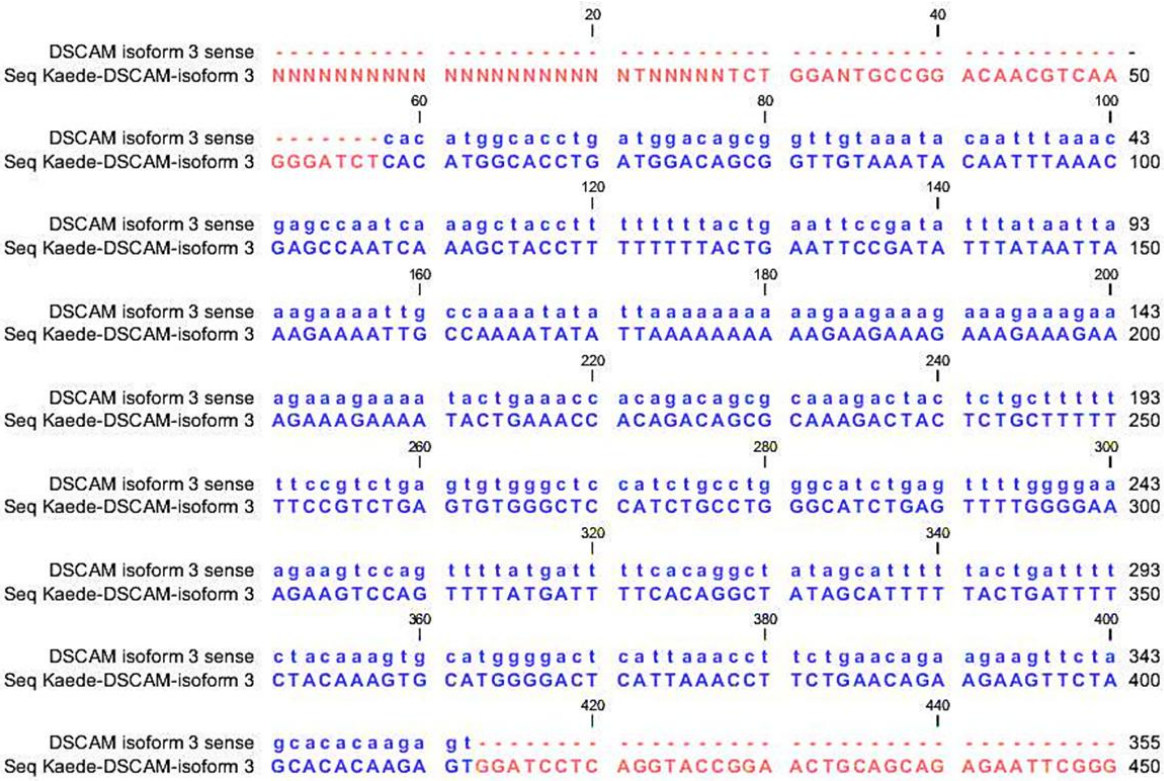

Alignment of DSCAM isoform 4 sequence with the constructed Kaede-DSCAM-isoform 4.

```
                                  20                  40
DSCAM isoform 4 sense     ---------- ---------- ---------- ---------- ----------
Seq Kaede-DSCAM-isoform 4 NNNNNNNNNN NNNNNNNNNN NNGTTNNNNN NTCTGGATTG CCGGACAACG 50
                      60                  80                  100
DSCAM isoform 4 sense     ---------- -cacatggca cctgatggac agcggttgta aatacaattt 39
Seq Kaede-DSCAM-isoform 4 TCAAGGGATC TCACATGGCA CCTGATGGAC AGCGGTTGTA AATACAATTT 100
                                 120                 140
DSCAM isoform 4 sense     aaacgagcca atcaaagcta cctttttttt actgaattcc gatatttata 89
Seq Kaede-DSCAM-isoform 4 AAACGAGCCA ATCAAAGCTA CCTTTTTTTT ACTGAATTCC GATATTTATA 150
                      160                 180                 200
DSCAM isoform 4 sense     attaaagaaa attgccaaaa tatattaaaa aaaaaagaag aaagaaagaa 139
Seq Kaede-DSCAM-isoform 4 ATTAAAGAAA ATTGCCAAAA TATATTAAAA AAAAAAGAAG AAAGAAAGAA 200
                                 220                 240
DSCAM isoform 4 sense     agaaagaaag aaaatactga aaccacagac agcgcaaaga ctactctgct 189
Seq Kaede-DSCAM-isoform 4 AGAAAGAAAG AAAATACTGA AACCACAGAC AGCGCAAAGA CTACTCTGCT 250
                      260                 280                 300
DSCAM isoform 4 sense     ttttttccgt ctgagtgtgg gctccatctg cctgggcatc tgagttttgg 239
Seq Kaede-DSCAM-isoform 4 TTTTTTCCGT CTGAGTGTGG GCTCCATCTG CCTGGGCATC TGAGTTTTGG 300
                                 320                 340
DSCAM isoform 4 sense     ggaaagaagt ccagttttat gattttcaca ggctatagca ttttttactga 289
Seq Kaede-DSCAM-isoform 4 GGAAAGAAGT CCAGTTTTAT GATTTTCACA GGCTATAGCA TTTTTACTGA 350
                      360                 380                 400
DSCAM isoform 4 sense     ttttctacaa agtgcatggg gactcattaa accttctgaa cagaagaagt 339
Seq Kaede-DSCAM-isoform 4 TTTTCTACAA AGTGCATGGG GACTCATTAA ACCTTCTGAA CAGAAGAAGT 400
                                 420                 440
DSCAM isoform 4 sense     tctagcacac aagagtaaaa aaaggaaacg gggggaacta gcctatttgt 389
Seq Kaede-DSCAM-isoform 4 TCTAGCACAC AAGAGTAAAA AAAGGAAACG GGGGGAACTA GCCTATTTGT 450
                      460                 480                 500
DSCAM isoform 4 sense     gaatcgaaga gggacgttga cgtgggggca ggggacagct tccgtcacct 439
Seq Kaede-DSCAM-isoform 4 GAATCGAAGA GGGACGTTGA CGTGGGGGCA GGGGACAGCT TCCGTCACCT 500
                                 520                 540
DSCAM isoform 4 sense     cgcacacctt tccttcccac taggaaccag gccctcggtt tgattttctg 489
Seq Kaede-DSCAM-isoform 4 CGCACACCTT TCCTTCCCAC TAGGAACCAG GCCCTCGGTT TGATTTTCTG 550
                      560                 580                 600
DSCAM isoform 4 sense     ttgttaatca ggatgagtgc tgtcagtgag ggggtggggt gggggggaatc 539
Seq Kaede-DSCAM-isoform 4 TTGTTAATCA GGATGAGTGC TGTCAGTGAG GGGGTGGGGT GGGGGGAATC 600
                                 620                 640
DSCAM isoform 4 sense     cattcggttt tctttttgtt tatttttttaa tttgatgaga cactctttgc 589
Seq Kaede-DSCAM-isoform 4 CATTCGGTTT TCTTTTTGNN TATTNNTTAN TTTGATGANA CACTCTTTGC 650
                      660                 680                 700
DSCAM isoform 4 sense     attttgtcta agcgaaataa aagagaaaag gtggtctgcc tt--------- 631
Seq Kaede-DSCAM-isoform 4 NTTTTGTCTA NNNNAAATAT AANAGAAAAG GTGGNCTGNN NNNGGATCCT 700
                                 720
DSCAM isoform 4 sense     ---------- ---------- -------t 632
Seq Kaede-DSCAM-isoform 4 CNNGNACTNN ANCNGCNNNN NNNNNNNT 728
```

Alignment of DSCAM isoform 5 sequence with the constructed Kaede-DSCAM-isoform 5.

```
                                    20                  40
DSCAM isoform 5 sense       ---------- ---------- ---------- ---------- ---------- -
Seq Kaede-DSCAM-isoform 5 sense NNNNNNNNNN NNNNNNNNNG TTNGNNNNNC TGGANTGCCG GACAACGTCA 50

                  60                  80                  100
DSCAM isoform 5 sense       ---------ca catggcacct gatggacagc ggttgtaaat acaatttaaa 42
Seq Kaede-DSCAM-isoform 5 sense AGGGATCTCA CATGGCACCT GATGGACAGC GGTTGTAAAT ACAATTTAAA 100

                                    120                 140
DSCAM isoform 5 sense       cgagccaatc aaagctacct tttttttact gaattccgat atttataatt 92
Seq Kaede-DSCAM-isoform 5 sense CGAGCCAATC AAAGCTACCT TTTTTTTACT GAATTCCGAT ATTTATAATT 150

                  160                 180                 200
DSCAM isoform 5 sense       aaagaaaatt gccaaaatat attaaaaaaa aaagaagaaa gaaagaaaga 142
Seq Kaede-DSCAM-isoform 5 sense AAAGAAAATT GCCAAAATAT ATTAAAAAAA AAAGAAGAAA GAAAGAAAGA 200

                                    220                 240
DSCAM isoform 5 sense       aagaaagaaa atactgaaac cacagacagc gcaaagacta ctctgctttt 192
Seq Kaede-DSCAM-isoform 5 sense AAGAAAGAAA ATACTGAAAC CACAGACAGC GCAAAGACTA CTCTGCTTTT 250

                  260                 280                 300
DSCAM isoform 5 sense       tttccgtctg agtgtgggct ccatctgcct gggcatctga gttttgggga 242
Seq Kaede-DSCAM-isoform 5 sense TTTCCGTCTG AGTGTGGGCT CCATCTGCCT GGGCATCTGA GTTTTGGGGA 300

                                    320                 340
DSCAM isoform 5 sense       aagaagtcca gttttatgat tttcacaggc tatagcattt ttactgattt 292
Seq Kaede-DSCAM-isoform 5 sense AAGAAGTCCA GTTTTATGAT TTTCACAGGC TATAGCATTT TTACTGATTT 350

                  360                 380                 400
DSCAM isoform 5 sense       tctacaaagt gcatggggac tcattaaacc ttctgaacag aagaagttct 342
Seq Kaede-DSCAM-isoform 5 sense TCTACAAAGT GCATGGGGAC TCATTAAACC TTCTGAACAG AAGAAGTTCT 400

                                    420                 440
DSCAM isoform 5 sense       agcacacaag agtaaaaaaa ggaaacgggg ggaactagcc tatttgtgaa 392
Seq Kaede-DSCAM-isoform 5 sense AGCACACAAG AGTAAAAAAA GGAAACGGGG GGAACTAGCC TATTTGTGAA 450

                  460                 480                 500
DSCAM isoform 5 sense       tcgaagaggg acgttgacgt gggggcaggg gacagcttcc gtcacctcgc 442
Seq Kaede-DSCAM-isoform 5 sense TCGAAGAGGG ACGTTGACGT GGGGGCAGGG GACAGCTTCC GTCACCTCGC 500

                                    520                 540
DSCAM isoform 5 sense       acacctttcc ttcccactag gaaccaggcc ctcggtttga ttttctgttg 492
Seq Kaede-DSCAM-isoform 5 sense ACACCTTTCC TTCCCACTAG GAACCAGGCC CTCGGTTTGA TTTTCTGTTG 550

                  560                 580                 600
DSCAM isoform 5 sense       ttaatcagga tgagtgctgt cagtgagggg gtggggtggg gggaatccat 542
Seq Kaede-DSCAM-isoform 5 sense TTAATCAGGA TGAGTGCTGT CAGTGAGGGG GTGGGGTGGG GGGAATCCAT 600

                                    620                 640
DSCAM isoform 5 sense       tcggttttct ttttgtttat tttttaattt gatgagacac tctttgcatt 592
Seq Kaede-DSCAM-isoform 5 sense TCGGTTTTCT TTTTGTTTAT TTTTTAATTT GATGAGACAC TCTTTGCATT 650

                  660                 680                 700
DSCAM isoform 5 sense       ttgtctaagc gaaataaaag agaaa-aggt ggtctgcctt tatttgcatg 641
Seq Kaede-DSCAM-isoform 5 sense TTGTCTAAGC GAAATAAANN ANNAANAGGT GGNCTGCCTT TATTTGCATG 700

                                    720                 740
DSCAM isoform 5 sense       tctactgata cctccctatc cattgctcgg gcctccttcc tgttcatatt 691
Seq Kaede-DSCAM-isoform 5 sense NCTACTGATA CCTCNNTATC CATTGCTCGG GCCTCCTTCC TGTTCATATN 750

                  760                 780                 800
DSCAM isoform 5 sense       gg-tgtttgt gaacaaaatg gctggaccca gtgcccaatc taggaaaaag 740
Seq Kaede-DSCAM-isoform 5 sense GNNTGTTTGT GAACAAAATG NCTGGANCNN -TGCCCANTC TNNNANANAN 799

                                    820                 840
DSCAM isoform 5 sense       atgctaagtt ttgaacagct caggtgttgc tgggaagaga caagaagata 790
Seq Kaede-DSCAM-isoform 5 sense ATGCNNANNT TT-------- ---------- ---------- ---------- 811

                  860                 880                 900
DSCAM isoform 5 sense       caacatcaac tccatggatg gaaaccacac caaaggcagc ctggtctccg 840
Seq Kaede-DSCAM-isoform 5 sense ---------- ---------- ---------- ---------- ---------- 811
```